

# Understanding Structural Isomerization during Ruthenium-Catalyzed Olefin Metathesis: A Deuterium Labeling Study

Florence C. Courchay, John C. Sworen, Ion Ghiviriga, Khalil A. Abboud, and Kenneth B. Wagener\*

The George and Josephine Butler Polymer Research Laboratory, Department of Chemistry, University of Florida, Gainesville, Florida 32611

Received November 17, 2005

A deuterium labeling study was undertaken to determine the mechanism of olefin isomerization during the metathesis reactions catalyzed by a second-generation Grubbs catalyst (**2**). The reaction of allyl-1,1- $d_2$  methyl ether with **2** at 35 °C was followed by  $^1\text{H}$  and  $^2\text{H}$  NMR spectroscopy. The evidence of deuterium incorporation at the C-2 position of the isomerized product, *trans*-propenyl methyl ether, led to the conclusion that a metal hydride addition–elimination mechanism was operating under these conditions. Consequently, complex **8**, an analogue of **2** bearing deuterated *o*-methyl groups on the aromatic rings of the NHC ligand, was synthesized to investigate the role of the NHC ligand in the formation of hydride species. Thermal decomposition of benzylidene **8** and methylidene **8'** was monitored by  $^2\text{H}$  NMR spectroscopy; no deuteride complex was detected in either case. The decomposition mixtures were tested for isomerization activity with benchmark 1-octene but did not match the isomerization rates observed with **2** under similar metathesis conditions. Reaction of complex **8** with various olefinic substrates not only confirmed the formation of a deuteride complex but also revealed the existence of a competitive H/D exchange process between the  $\text{CD}_3$  groups on the NHC ligand and the C–H bonds of the substrate. We propose that the exchange is promoted by a ruthenium dihydride intermediate whose formation is closely related to the methylidene decomposition.

## Introduction

The discovery of well-defined, functional-group-tolerant ruthenium carbene catalysts such as Grubbs'  $(\text{PCy}_3)_2(\text{Cl})_2\text{Ru}=\text{CHPh}$  (**1**)<sup>1</sup> has considerably broadened the scope of olefin metathesis.<sup>2</sup> The versatility of this class of catalysts has contributed to their growing popularity and motivated new developments. A “second generation” of catalytic systems was introduced as one N-heterocyclic carbene replaced a phosphine ligand (**2** and **3** in Figure 1), further enhancing their catalytic activity and the thermal stability.<sup>3,4</sup> Since then, many ligand

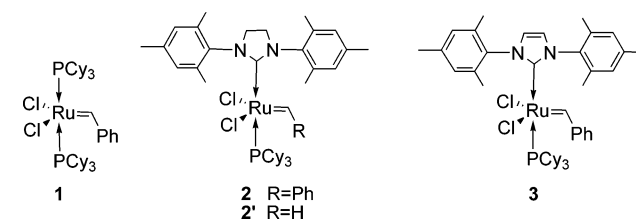


Figure 1. Olefin metathesis catalysts.

modifications have been reported in order to tune the activity and/or the stability of the catalyst according to specific reaction conditions. For example, the exchange of a phosphine for an isopropoxy-tethered benzylidene conferred an exceptional stability to the catalyst in solution, which has allowed the catalyst to be recycled after ring-closing metathesis (RCM) or cross-metathesis (CM) reactions.<sup>5</sup> Also, addition of more labile ligands, such as pyridine derivatives, enabled fast initiation rates particularly desirable for living ring-opening metathesis polymerization (ROMP).<sup>6</sup>

However, in addition to their high reactivity in metathesis chemistry, these ruthenium catalysts have been shown to undergo non-metathesis transformations.<sup>7</sup> Among them, alkene isomerization has emerged as an important side reaction of

\* To whom correspondence should be addressed. E-mail: wagener@chem.ufl.edu.

(1) (a) Schwab, P.; Grubbs, R. H.; Ziller, J. *J. Am. Chem. Soc.* **1996**, *118*, 100–110. (b) Dias, E. L.; Nguyen, S. T.; Grubbs, R. H. *J. Am. Chem. Soc.* **1997**, *119*, 3887–3897. (c) Ulman, M.; Grubbs, R. H. *Organometallics* **1998**, *17*, 2484–2489. (d) Ulman, M.; Grubbs, R. H. *J. Org. Chem.* **1999**, *64*, 7202–7207.

(2) For relevant reviews, see: (a) *Handbook of Metathesis*; Grubbs, R. H., Ed.; Wiley-VCH: Weinheim, Germany, 2003. (b) Trnka, T. M.; Grubbs, R. H. *Acc. Chem. Res.* **2001**, *34*, 18–29. (c) Fürstner, A. *Angew. Chem., Int. Ed.* **2000**, *39*, 3012–3043. (d) Grubbs, R. H.; Chang, S. *Tetrahedron* **1998**, *54*, 4413–4450. (e) Schuster, M.; Blechert, S. *Angew. Chem., Int. Ed.* **1997**, *36*, 2036–2056. (f) Armstrong, S. K. *J. Chem. Soc., Perkin Trans. I* **1998**, 371–388. (g) Frenzel, U.; Nuyken, O. *J. Polym. Sci.: Chem.* **2002**, *40*, 2895–2916.

(3) (a) Scholl, M.; Ding, S.; Lee, C.; Grubbs, R. H. *Org. Lett.* **1999**, *1*, 953–956. (b) Sanford, M. S.; Ulman, M.; Grubbs, R. H. *J. Am. Chem. Soc.* **2001**, *123*, 749–750. (c) Sanford, M. S.; Love, J. A.; Grubbs, R. H. *J. Am. Chem. Soc.* **2001**, *123*, 6543–6554.

(4) (a) Scholl, M.; Trnka, T. M.; Morgan, J. P.; Grubbs, R. H. *Tetrahedron Lett.* **1999**, *40*, 2247–2250. (b) Weskamp, T.; Kohl, F. J.; Herrmann, W. A. *J. Organomet. Chem.* **1999**, *582*, 362–365. (c) Ackermann, L.; Fürstner, A.; Westcamp, T.; Kohl, F. J.; Herrmann, W. A. *Tetrahedron Lett.* **1999**, *40*, 4787–4790. (d) Huang, J.; Stephens, E. D.; Nolan, S. P.; Pedersen, J. L. *J. Am. Chem. Soc.* **1999**, *121*, 2674–2678.

(5) (a) Kingsbury, J. S.; Harrity, J. P. A.; Bonitatebus, P. J.; Hoveyda, A. H. *J. Am. Chem. Soc.* **1999**, *121*, 791–799. (b) Garber, S. B.; Kingsbury, J. S.; Gray, B. L.; Hoveyda, A. H. *J. Am. Chem. Soc.* **2000**, *122*, 8168–8179. (c) For a review on Ru-bearing bidentate carbenes: Hoveyda, A. H.; Gillingham, D. G.; Van Veldhuizen, J. J.; Kataoka, O.; Garber, S. B.; Kingsbury, J. S.; Harrity, J. P. A. *Org. Biomol. Chem.* **2004**, *2*, 8–23.

(6) (a) Love, J. A.; Morgan, J. P.; Trnka, T. M.; Grubbs, R. H. *Angew. Chem., Int. Ed.* **2002**, *41*, 4035–4037. (b) Love, J. A.; Sanford, M. S.; Day, M. W.; Grubbs, R. H. *J. Am. Chem. Soc.* **2003**, *125*, 10103–10109.

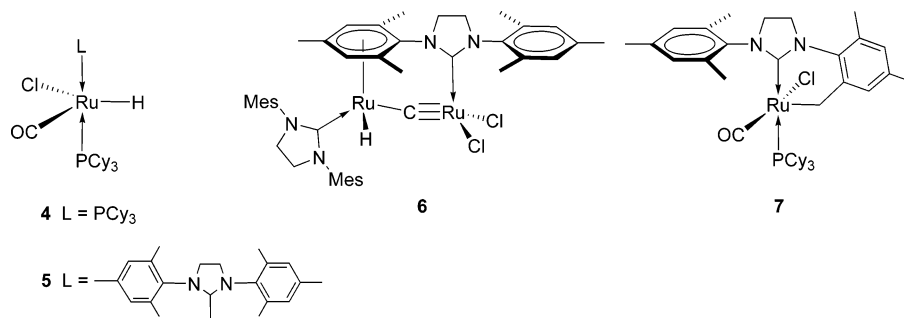


**Figure 2.** Decomposition products of ruthenium carbene complexes.

ruthenium-catalyzed metathesis, disturbing the product's microstructure by apparent migration of the double bond along the alkyl chain.<sup>8</sup> First observed on substrates containing allylic functionalities in combination with first-generation catalysts,<sup>9</sup> double-bond isomerization has since been reported with second-generation catalysts on a broad variety of substrates competitively, sometimes prior to olefin metathesis.<sup>10,11</sup> Promoted by diverse transition metals, olefin isomerization has been known to operate through two distinctive pathways: either through  $\eta^3$ -allyls or through an alkyl intermediate involving a long-lived metal hydride.<sup>12</sup> Mechanistically, the  $\pi$ -allyl involves a formal *intramolecular* 1,3-H shift, while the metal hydride operates through an *intermolecular* addition–elimination with an inherently competitive 1,2-H shift. Consequently, isotopic labeling experiments have often been used to probe the nature of the mechanism.<sup>13</sup> However, despite the increasing number of studies, the ruthenium intermediate responsible for this undesirable reaction has not been identified yet. Although isomerization is often attributed to the formation of a ruthenium hydride *in situ*, as a decomposition product of the original carbene catalyst,<sup>14</sup> the possibility of a  $\pi$ -allyl mechanism cannot be ruled out.<sup>10d</sup>

Apart from standard hydrogenolysis,<sup>15</sup> numerous pathways have been proposed for the transformation of ruthenium carbene into ruthenium hydride complexes. For example, the carbonyl hydrides **4** and **5** (Figure 2), first isolated during the decomposition of alkoxycarbene complexes,<sup>16</sup> were identified as products of the reaction of **1** and **2** with primary alcohols in the presence of a base.<sup>17</sup> Although the mechanism is still at a speculative stage,<sup>16a,17a</sup> both complexes are known to be efficient catalysts for isomerization, hydrogenation,<sup>17,18</sup> and hydrovinylation.<sup>19</sup> More recently, Grubbs has isolated the dinuclear ruthenium hydride **6** as one of the decomposition products of the methylidene intermediate **2'**, formed during a metathesis cycle.<sup>20</sup> Other studies include the possibility of ruthenium insertion into the C–H bond of one of the methyl groups present on the NHC ligand.<sup>17d,21</sup> This type of activation is common for complexes containing NHC ligands and has been witnessed during the preparation of ruthenium carbene **2**; however, it has not yielded the hydride complex **7**.<sup>17d</sup>

Acyclic diene metathesis (ADMET) has been used recently for the modeling of precise ethylene/ $\alpha$ -olefin copolymers.<sup>22</sup> Therefore controlling isomerization is crucial, since it results in irregular microstructures, whether it occurs on the monomer or on the product (Figure 3). Previously, we have reported the metathesis vs isomerization activity of ruthenium carbene catalysts using the model substrate 1-octene.<sup>11</sup> Even though

(7) (a) For a review on non-metathetic behavior of Ru carbenes, see: Alcaide, B.; Almendros, P. *Chem. Eur. J.* **2003**, *9*, 1258–1262. (b) Schmidt, B.; Pohler, M.; Costisella, B. *J. Org. Chem.* **2004**, *69*, 1421–1424. (c) Faulkner, J.; Edlin, C. D.; Fengas, D.; Preece, I.; Quayle, P.; Richards, S. N. *Tetrahedron Lett.* **2005**, *46*, 2381–2385. (d) Edlin, C. D.; Faulkner, J.; Fengas, D.; Knight, C. K.; Parker, J.; Preece, I.; Quayle, P.; Richards, S. N. *Synlett* **2005**, *4*, 572–577. (e) Hoye, T. R.; Zhao, H. *Org. Lett.* **1999**, *1*, 169–171. (f) Gurjar, M. K.; Yakambram, P. *Tetrahedron Lett.* **2001**, *42*, 3633–3636.

(8) For a short review on the isomerization behavior of ruthenium carbenes, see: Schmidt, B. *Eur. J. Org. Chem.* **2004**, *9*, 1865–1880.

(9) (a) Miller, S. J.; Blackwell, H. E.; Grubbs, R. H. *J. Am. Chem. Soc.* **1996**, *118*, 9606–9614. (b) Maynard, H. D.; Grubbs, R. H. *Tetrahedron Lett.* **1999**, *40*, 4137–4140. (c) Bourgeois, D.; Pancrazi, A.; Ricard, L.; Prunet, J. *Angew. Chem.* **2000**, *112*, 742–744; *Angew. Chem., Int. Ed.* **2000**, *39*, 725–728. (d) Edwards, S. D.; Lewis, T.; Taylor, R. J. K. *Tetrahedron Lett.* **1999**, *40*, 4267–4270. (e) Schmidt, B.; Wildemann, H. *J. Org. Chem.* **2000**, *65*, 5817–5822.

(10) (a) Fürstner, A.; Thiel, O. R.; Ackermann, L.; Schanz, H.-J.; Nolan, S. P. *J. Org. Chem.* **2000**, *65*, 2204–2207. (b) Cadot, C.; Dalko, P. I.; Cossy, J. *Tetrahedron Lett.* **2002**, *43*, 1839–1841. (c) Sutton, A. E.; Seigal, B. A.; Finnegan, D. F.; Snapper, M. L. *J. Am. Chem. Soc.* **2002**, *124*, 13390–13391. (d) Bourgeois, D.; Pancrazi, A.; Nolan, S. P.; Prunet, J. *J. Org. Chem.* **2002**, *67*, 643–644, 247–252. (e) Sworen, J. C.; Pawlow, J. H.; Case, W.; Lever, J.; Wagener, K. B. *J. Mol. Catal.* **2002**, *194*, 69–78.

(11) (a) Lehman, S. E.; Schwendeman, J. E.; O'Donnell, P. M.; Wagener, K. B. *Inorg. Chim. Acta* **2002**, *345*, 190–198. (b) Courchay, F. C.; Sworen, J. C.; Wagener, K. B. *Macromolecules* **2003**, *36*, 8231–8239.

(12) Crabtree, R. H. *The Organometallic Chemistry of the Transition Metals*, 2nd ed.; Wiley: New York, 1994.

(13) (a) Hendrix, W. T.; Cowherd, F. G.; von Rosenberg, J. L. *Chem. Commun.* **1968**, 97–99. (b) Bergens, S. H.; Bosnich, B. *J. Am. Chem. Soc.* **1991**, *113*, 958–967. (c) McGrath, D. V.; Grubbs, R. H. *Organometallics* **1994**, *13*, 224–235. (d) Baudry, D.; Ephritikhine, M.; Felkin, H. *J. Chem. Soc., Chem. Commun.* **1978**, 694–695. (e) Clark, H. C.; Kurosawa, H. *Inorg. Chem.* **1973**, *12*, 1566–1569. (f) Casey, C. P.; Cyr, C. R. *J. Am. Chem. Soc.* **1973**, *95*, 2248–2253.

(14) For relevant reviews on the reactivity of ruthenium hydride complexes, see: (a) Naota, T.; Takaya, H.; Murahashi, S. *Chem. Rev.* **1998**, *98*, 2599–2660. (b) Trost, B. M.; Toste, F. D.; Pinkerton, A. B. *Chem. Rev.* **2001**, *101*, 2067–2096.

(15) (a) Drouin, S. D.; Yap, G. P. A.; Fogg, D. E. *Inorg. Chem.* **2000**, *39*, 5412–5414. (b) Fogg, D. E.; Drouin, S. D.; Zamanian, F. U.S. Pat. Appl. 60/192394, priority date March 26, 2000. (c) Beatty, R. P.; Paciello, R. A. U.S. Patent 5,554,778, 1996.

(16) (a) Wu, Z.; Nguyen, S. T.; Grubbs, R. H.; Ziller, J. W. *J. Am. Chem. Soc.* **1995**, *117*, 5503–5511. (b) Louie, J.; Grubbs, R. H. *Organometallics* **2002**, *21*, 2153–2164.

(17) (a) Dinger, M. B.; Mol, J. C. *Organometallics* **2003**, *22*, 1089–1095. (b) Dinger, M. B.; Mol, J. C. *Eur. J. Inorg. Chem.* **2003**, 2827–2833. (c) Banti, D.; Mol, J. C. *J. Organomet. Chem.* **2004**, *689*, 3113–3116. (d) Trnka, T. M.; Morgan, J. P.; Sanford, M. S.; Wilhelm, T. E.; Scholl, M.; Choi, T.-L.; Ding, S.; Day, M. D.; Grubbs, R. H. *J. Am. Chem. Soc.* **2003**, *125*, 2546–2558.

(18) (a) Yi, C. S.; Lee, D. W. *Organometallics* **1999**, *18*, 5152–5156. (b) Yi, C. S.; Lee, D. W.; He, Z.; Rheingold, A. L.; Lam, K.-C.; Concolino, T. E. *Organometallics* **2000**, *19*, 2909–2915. (c) Lee, H. M.; Smith, D. C.; Zhengjie, H.; Stevens, E. D.; Yi, C. S.; Nolan, S. P. *Organometallics* **2001**, *20*, 794–797. (d) Dharmasena, U. L.; Foucault, H. M.; dos Santos, E. N.; Fogg, D. E.; Nolan, S. P. *Organometallics* **2005**, *24*, 1056–1058.

(19) Esteruelas, M. A.; Werner, H. *J. Organomet. Chem.* **1986**, *303*, 221–231.

(20) Hong, S. H.; Day, M. W.; Grubbs, R. H. *J. Am. Chem. Soc.* **2004**, *126*, 7414–7415.

(21) Jazsar, R. F. R.; Macgregor, S. A.; Mahon, M. F.; Richards, S. P.; Whittlesey, M. K. *J. Am. Chem. Soc.* **2002**, *124*, 4944–4945.

(22) (a) Wagener, K. B.; Valenti, D. J.; Hahn, S. F. *Macromolecules* **1997**, *30*, 6688–6690. (b) Smith, J. A.; Brzezinska, K. R.; Valenti, D. J.; Wagener, K. B. *Macromolecules* **2000**, *33*, 3781–3794. (c) Sworen, J. C.; Smith, J. A.; Berg, J. M.; Wagener, K. W. *J. Am. Chem. Soc.* **2004**, *126*, 11238–11246.

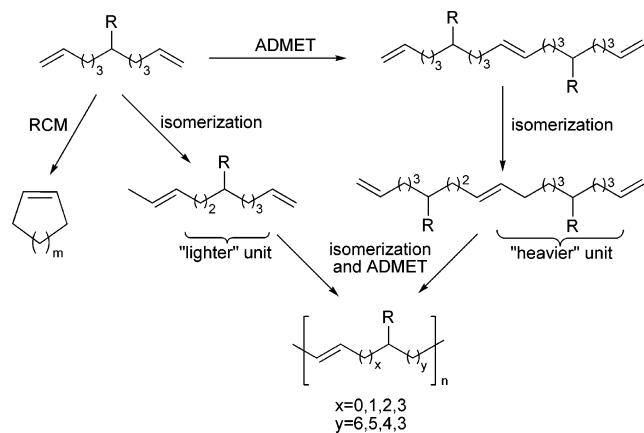


**Figure 3.** Effect of isomerization during ADMET polymerization.

metathesis consistently occurred more quickly, isomerization products could represent as much as 80% of the reaction mixture with catalysts containing NHC ligands. When other modified complexes were used, we observed that the isomerization activity was closely related to the metathesis activity.<sup>23</sup> Intrigued by the apparent relationship between isomerization and metathesis behavior, we decided to investigate the mechanism of isomerization under metathesis conditions. The reaction of allyl-1,1-*d*<sub>2</sub> methyl ether with catalyst **2** was monitored by <sup>1</sup>H and <sup>2</sup>H NMR spectroscopy to examine deuterium scrambling and therefore determine the operating isomerization mechanism. We also designed a deuterated version of catalyst **2** (complex **8** in Scheme 1) to further demonstrate the role of the NHC ligand in catalyst decomposition and assess the possibility of C–H activation, which could be responsible for the formation of a metal hydride complex. Again, we used <sup>2</sup>H NMR to monitor the decomposition of complex **8** and observe its behavior in the presence of olefinic substrates, looking for any deuterium incorporation that would confirm the presence of a ruthenium deuteride complex.

## Results and Discussion

**Mechanistic Studies.** Even though both the  $\pi$ -allyl hydride and the metal hydride addition–elimination mechanism result in the same product, isotopic labeling studies can highlight their differences. Indeed, the two pathways can be distinguished by looking at the hydrogen shift undergone during the isomerization reaction. The  $\pi$ -allyl mechanism, involving a metal with two empty coordination sites that does not contain a hydride ligand, is typically *intramolecular*. A free olefin coordinates to the metal and undergoes an oxidative addition of the allylic C–H bond to form a  $\pi$ -allyl metal hydride intermediate. The hydride fragment is then transferred to the terminal position (of an  $\alpha$ -olefin) by reductive elimination to yield the isomerized olefin. Hence, a formal 1,3-*H* shift is observed when the  $\pi$ -allyl mechanism is active (Figure 4).

On the other hand, the metal hydride mechanism involves a distinct metal hydride complex already present in the reaction and is therefore *intermolecular*: i.e., hydrogen atoms from one substrate can be transferred to the catalyst onto another substrate molecule. The olefin inserts into the metal–hydride bond to form either a primary metal alkyl (thermodynamically favored) or a secondary metal alkyl that will lead to the isomerized olefin by  $\beta$ -H elimination, generating another metal hydride. The occurrence of both Markovnikov and anti-Markovnikov addi-

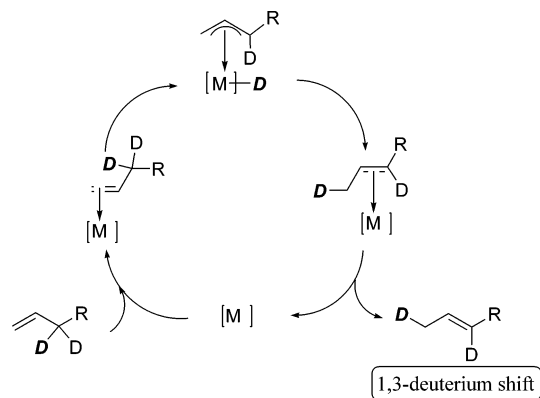


**Figure 4.** Deuterium shift with a  $\pi$ -allyl hydride mechanism.

tions of the metal hydride across the double bond results in a characteristic 1,2-*H* shift.<sup>13c</sup> When a primary metal alkyl undergoes a  $\beta$ -elimination of a different hydrogen, the resulting olefin can reinsert in the metal–hydride bond to form a secondary metal alkyl. Subsequent  $\beta$ -elimination of the appropriate hydrogen results in an apparent 1,2-*H* shift, as illustrated in Figure 5 for a deuterated olefin. A formal 1,3-*H* shift can also be observed through the formation of a secondary metal-hydride.

Substrates such as allyl-1,1-*d*<sub>2</sub> alcohol<sup>13a–c</sup> and the corresponding methyl ether<sup>13c–e</sup> have often been used to probe the nature of the hydrogen shift in metal-catalyzed olefin isomerization, particularly because of the irreversibility of the reaction. Indeed, allyl-1,1-*d*<sub>2</sub> alcohol will isomerize exclusively into propionaldehyde-1,3-*d*<sub>2</sub> in the case of a  $\pi$ -allyl hydride mechanism, while a mixture of partially deuterated propionaldehydes with deuterium incorporation at the C-2 position will be expected in the case of the metal hydride mechanism. Actually this method is often taken as evidence for the  $\pi$ -allyl hydride mechanism without investigating the inter-/intramolecularity of the process.

In the present case, allyl alcohol has been known to react with ruthenium carbenes and form hydride complexes.<sup>7d,e,24</sup> Therefore, we have worked with allyl methyl ether only, which in the end should provide us with the same set of observations. A 2.3 M solution of allyl-1,1-*d*<sub>2</sub> methyl ether (**9**) in C<sub>6</sub>D<sub>6</sub> was charged in an airtight NMR tube with 0.2 mol % of complex **2** and heated at 35 °C for 3 days to reproduce the conditions used in previous isomerization studies.<sup>11</sup> The composition of the reaction mixture was identified using 2D NMR and NOE experiments.<sup>25</sup> The resulting sample consists of the four compounds shown in Figure 6: *cis*- and *trans*-propenyl methyl ether (**10cis** and **10trans**) are the isomerization products of the starting material and represent 70% of the mixture; the remaining 30%, *cis*- and *trans*-1,4-dimethoxybut-1-ene (**11cis** and **11trans**), are the result of isomerization on the metathesis product. Each of these compounds is a mixture of the four isotopomers derived from partial deuteration in positions 2 and 3 of the alkylene ether. Interestingly, position 1 is completely deuterated, while position 4 does not contain any deuterium. The relative ratios of each compound and the molar fractions of deuteration in each position are given in Figure 6.<sup>26</sup>

The facts that only four products are present, that position 1 is fully deuterated, and that position 4 is not deuterated at all provide good evidence against deuterium exchange with the

(24) Werner, H.; Grunwald, C.; Stuer, W.; Wolf, J. *Organometallics* **2003**, *22*, 1558–1560.

(25) The details of NMR and NOE experiments are available in the Supporting Information.

(23) Courchay, F. C. Ph.D. Dissertation, University of Florida, 2005.

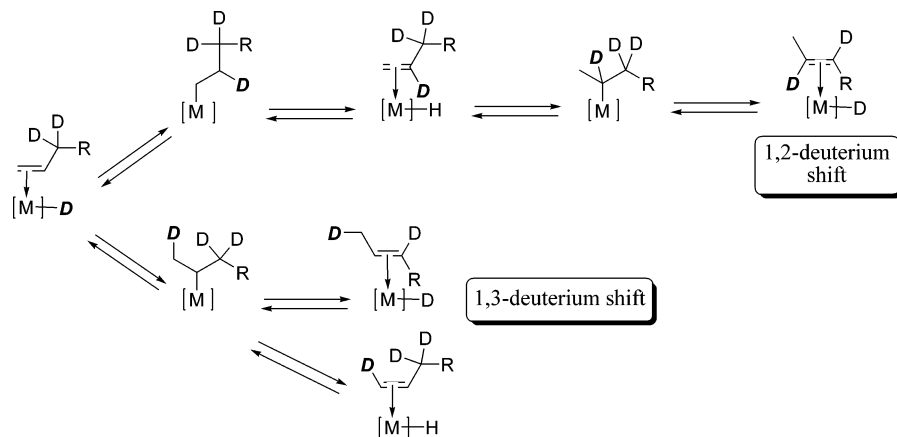


**Figure 5.** Deuterium shifts with a metal hydride addition–elimination mechanism.

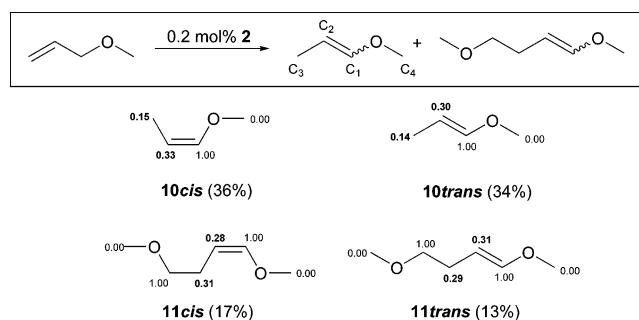


**Figure 6.** Products of the reaction of allyl-1,1- $d_2$  methyl ether with complex **2**. The molar fractions of each compound are given in parentheses; the molar fractions of deuterium are indicated at each position.

solvent: i.e., all the deuterium present on the products actually comes from the starting material, which confirms the validity of this model study. Therefore, deuterium incorporation at the C-2 position clearly indicates that the *isomerization mechanism operating here is a metal hydride addition–elimination*. In fact, the relative ratios of deuterium incorporation at positions 2 and 3 reflect the relative rates of Markovnikov (formation of a secondary metal alkyl) versus anti-Markovnikov addition (formation of a primary metal alkyl) of the metal hydride across the olefin bond (Figure 6). This ratio is estimated to be about 1:2 for both **10cis** and **10trans**, which is consistent with the preferred formation of the thermodynamically favored primary metal alkyl. For example, Cramer et al. reported that in the isomerization of 1-butene by rhodium(III) hydride, addition of D to C-2 was 15 times faster than addition to C-3.<sup>27</sup> The lower ratio obtained with our allyl ether may be a result of the directing effect of the oxygen moiety, as described previously by McGrath and Grubbs during the isomerization of allylic alcohols and ethers by  $\text{Ru}^{\text{II}}(\text{H}_2\text{O})_6(\text{tos})_2$ .<sup>13c</sup>

In the case of **11cis** and **11trans**, the relative ratios of deuterium incorporation at C-2 and C-3 are approximately 1:1, which makes sense, since isomerization occurs on an internal double bond. Indeed, the metal hydride can only add across the olefin bond of the metathesis product and forms exclusively a secondary metal alkyl.

The complete deuteration of position 1 suggests the irreversibility of the isomerization reaction. The kinetic product is

(26) The sum of deuterium for each molecule of product **9** and **10** does not equal 2.00 (number of deuteriums present in one molecule of allyl-1,1- $d_2$  methyl ether) because some deuterium atoms were incorporated in the ethylene released during the metathesis of allyl-1,1,3- $d_3$  methyl ether. (27) Cramer, R. *J. Am. Chem. Soc.* **1966**, *88*, 2272–2282.

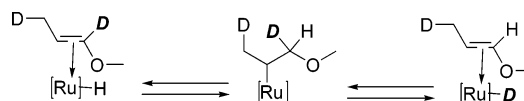


**Figure 7.** Incorporation of hydrogen at C-1 by reversible isomerization.

formed, and its formation is expected to be thermodynamically irreversible, as it is a vinyl ether. In any case, if the reaction were reversible, an isomerized olefin, methoxy-1,3- $d_2$ -propene for instance, should be able to insert into a metal–hydride bond to form a secondary metal alkyl, which could subsequently undergo a  $\beta$ -D elimination to produce methoxy-3- $d$ -propene (Figure 7). This transfer of the methylene deuterium to the metal would automatically bring the percent deuteration at C-1 under 100%, which is not the case. A similar behavior was witnessed by Krompiec et al. with the hydride complex  $\text{RuClH}(\text{CO})(\text{PPh}_3)_3$ .<sup>28</sup> Under ADMET conditions, the reaction of the allylic ether *N,N*-bis[3-(allyloxy)-2-hydroxypropyl]aniline with **2** resulted in complete isomerization, leading to the vinylic ether.<sup>10e</sup>

The distribution of isomerization vs metathesis product is a result of several factors. Although metathesis is often believed to proceed more quickly and is therefore the primary reaction, our conditions are set up in a closed system, which limits its progression. Once the system is saturated with ethylene, it reaches equilibrium and metathesis chemistry virtually stops. Meanwhile, the isomerization reaction continues to consume starting material and produce a vinyl ether, which can then trap the metathesis catalyst into a stable, low-reactive Fischer carbene whose biphosphine analogue is known to thermally decompose into the hydride complex **5**.<sup>16</sup> *Observation of a typical color change from pink to bright yellow, indicative of alkoxy carbene decomposition, reinforces the argument for the proposed mechanism.* Thus, not only does the metathesis rate decrease over time but also the isomerization rate increases as the hydride concentration increases (if we consider that the source of hydride is related to catalyst decomposition). Hence, only 30% of metathesis product is formed and is subsequently isomerized to **10cis** and **10trans**.

**Other Mechanistic Considerations.** The olefin isomerization mechanism operating here cannot involve a  $\beta$ -H shift from an allylic proton to the metal, as proposed for the reaction of allyl alcohols in the presence of **1**.<sup>24</sup> Indeed, the mechanism shown in Figure 8 involves the stoichiometric consumption of the isomerization–metathesis catalyst and in our case would have yielded only up to 0.2 mol % of isomerized starting material.

(28) Krompiec, S.; Antoszczyszyn, M.; Urbala, M.; Bieg, T. *Pol. J. Chem.* **2000**, *74*, 737–741.

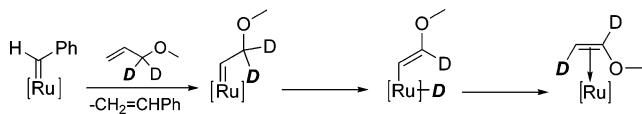


**Figure 8.**  $\beta$ -H abstraction–elimination mechanism proposed for the reaction of allyl alcohol with **1**.

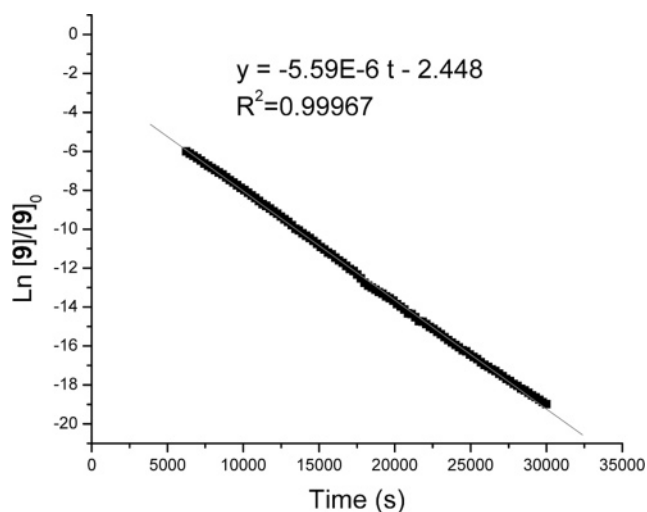


**Figure 9.** Total concentration of **9** versus time. Conditions: 2.3 M solution of **9** in  $C_6D_6$  with 0.2 mol % of **2** at 35 °C for 8 h.

Nevertheless, this step may be responsible for the formation of the hydride species involved in the metal hydride isomerization reaction described above, by reaction of the ruthenium carbene with vinyl ether, and subsequent decomposition of the Fischer carbene hence formed.<sup>16</sup>

**Kinetic Studies.** The relative rates of isomerization versus metathesis could be measured for allyl-1,1- $d_2$  methyl ether when the system had reached metathesis equilibrium. Indeed, when the reaction in a closed system was monitored by  $^1H$  NMR, the starting material quickly disappeared to form 1,4-dimethoxybut-2-ene,<sup>29</sup> but after 60 min, the rate of formation of metathesis product became slower until its concentration leveled, indicating metathesis equilibrium at only 7% conversion. From this point on, we clearly observed the steady formation of isomerized starting material. Considering the rate of metathesis to be negligible and the isomerization of **9** to be irreversible, as shown above, the isomerization reaction then followed first-order kinetics. The rate was calculated at approximately  $5.59 \times 10^{-6} s^{-1}$  (Figure 9). By considering the concentrations of metathesis product and starting material at equilibrium, the metathesis equilibrium constant could also be estimated at  $4.04 \times 10^{-6}$ ,<sup>30</sup> a small value that emphasizes the importance of ethylene removal.

Now that we know olefin isomerization is promoted by a metal hydride complex, the question remains: what is the structure of this hydride species, and what causes its formation? Realizing the complexity of the question, we first endeavored to understand the role of NHC ligands in the isomerization behavior of ruthenium carbene catalysts.

**Design, Synthesis, and Characterization.** Recent reports have shown that metathesis catalysts bearing NHC ligands undergo olefin isomerization to a considerable extent compared

to the case for their phosphine analogues.<sup>8,11</sup> Ligand variation experiments on both the phosphine and carbene ligands have further reinforced the idea that NHC ligands play a major role in the isomerization behavior of ruthenium carbene catalysts.<sup>23</sup> In light of the results discussed above, we decided to investigate the eventual participation of NHC groups in the production of a metal hydride. Speculations evoke a possible ruthenium insertion into the C–H bond of one of the mesityl groups. To address this issue, we built a complex that would be comparable to catalyst **2** in structure and reactivity and would simultaneously allow us to track its evolution through isotopic labeling experiments. Complex **8** (Scheme 1) was designed with fully deuterated *o*-methyl groups on the NHC aryl rings so that any sign of ruthenium insertion would be easily detected by NMR spectroscopy.

We started with bromo-*m*-xylene (**A**) and used an oxidation–reduction strategy to obtain the deuterated xylene **D**. Direct reduction of the diacid **B** by lithium aluminum deuteride only yielded unidentified decomposition products. The reaction was rendered successful by moving to the corresponding diester but still necessitated controlled conditions to reach reasonable yields (85%). The alcohol groups of **C** were substituted to bromine groups to allow further reduction to the fully deuterated bromoxylene **D**. Deuterated 2,6-dimethylaniline was obtained by substitution of the bromine group through a Grignard reaction with (trimethylsilyl)methyl azide (TMSDA). The corresponding ligand salt was then easily prepared according to the regular procedure. However, we used the chloroform adduct for the synthesis of the final complex **8**, to ensure a better yield and avoid salt contamination.<sup>17d</sup>

Both the  $^1H$  and  $^{31}P$  NMR spectra of complex **8** are very similar to those of catalyst **2**, showing the same carbene shift at 19.63 ppm and the same phosphine shift at 29.5 ppm.<sup>3a</sup> No hydride trace was detected at this point. The  $^2H$  NMR shows two singlets at 2.35 and 2.75 ppm, representing the aryl rings in the front (above the benzyldiene) and in the back (above the open coordination site) of the catalyst. Rotation of the NHC ring about the Ru–C bond is typically slow on the NMR time scale, as observed with the parent mesityl complex **2**, which exhibits four methyl resonances (in a 3:3:6:6 ratio) at low temperature. At room temperature the fluxional processes of the benzyldiene induce a broadening of the original signals into two singlets, as observed here. The crystal structure exhibits a typical square-pyramidal geometry with the carbene moiety in the apical position (Figure 10).<sup>31</sup> However, almost the entire molecule is affected with an inherent disorder related to the existence of two mirror images within the asymmetric unit. Representative bond lengths and angles of complexes **2** and **8** are reported in Table 1 for comparison.<sup>6b</sup> Apart from the chlorine atoms, whose bond lengths to ruthenium vary by about 0.1 Å, both solid-state structures appear to be very similar. The deviation of the chlorines is just a result of the global molecular disorder. In fact, the Ru–Cl bond length averages 2.3929 Å from the two disordered structures.<sup>32</sup> Since complexes **2** and **8** are so related structurally, it is reasonable to expect similar catalytic behavior.

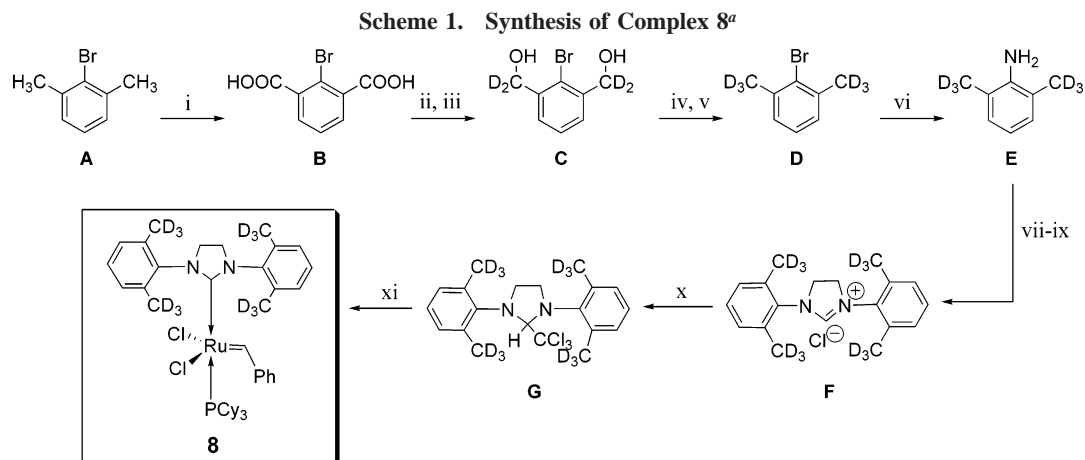
**Thermal Stability.** When a solution of complex **8** in benzene- $d_6$  was left at 70 °C in a sealed ampule, no sign of ruthenium deuteride was detected by  $^2H$  NMR, even after 21 days, when

(29) Traces of deuterium incorporation at the olefinic bond of the starting material were also observed, suggesting the presence of a metal hydride at this early stage of the reaction.

(30) Metathesis equilibrium constant  $K_M = [MP]_e[C_2H_4]_e/[SM]_e^2 = [MP]_e^2/[SM]_e^2$ , where MP is the metathesis product, 1,4-dimethoxybut-2-ene, and SM is the starting material, allyl-1,1- $d_2$  methyl ether.

(31) Crystals suitable for X-ray structure determination were obtained from slow diffusion of pentane into a saturated solution of **8** in benzene at room temperature.

(32) Crystal data for compound **8** are available as Supporting Information.



<sup>a</sup> Reagents and conditions: (i)  $\text{KMnO}_4$ , 50% *t*BuOH in water, reflux, 16 h (yield 99%); (ii)  $\text{K}_2\text{CO}_3$ ,  $\text{CH}_3\text{I}$ , cat.  $\text{CsCO}_3$ , DMF, reflux 12 h (yield 81%); (iii) LAD, THF, 0 °C, 20 min (yield 85%); (iv)  $\text{CBr}_4$ ,  $\text{PPh}_3$ ,  $\text{CH}_2\text{Cl}_2$  (yield 70%); (v) LAD, THF, room temperature (yield 90%); (vi) (a) Mg, ether, reflux, 2 h, (b) TMSDA, room temperature, 3 h (yield 55%); (vii) glyoxal, *n*PrOH, water, room temperature to 60 °C, 6 h (yield 80%); (viii)  $\text{NaBH}_4$ , 1:2 MeOH–THF, room temperature, 16 h, 1 M HCl (yield 85%); (ix)  $\text{CH}(\text{OEt})_3$ , reflux, 4 h (yield 60%); (x) NaH,  $\text{CHCl}_3$ , room temperature 2 h (yield 82%); (xi) **1**, toluene, 60 °C, 90 min (yield 75%).

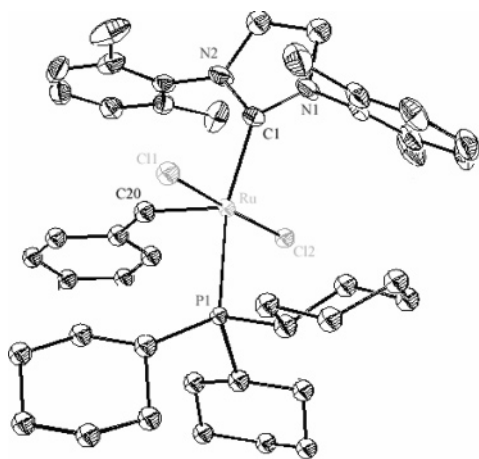


**Figure 10.** X-ray structure of complex **8**.

the decomposition process was already at an advanced stage.<sup>33</sup> In fact, observation of the  $^{31}\text{P}$  NMR spectrum indicates that only 4% of the original complex remained. Other typical peaks have emerged at 10.4, 34.6, 47.0, and 47.4 ppm, along with what appears to constitute 70% of the phosphorus products centered at around 72 ppm. The first signal can be attributed to free  $\text{PCy}_3$ . The peak at 34.6 ppm seems consistent with the phosphonium salt  $[\text{PCy}_3\text{CH}_2\text{Ph}]^+[\text{Cl}]^-$ , observed by Grubbs as a byproduct of methylidene **2'** decomposition.<sup>20</sup> Interestingly, we initially attributed the peaks at 47.0 and 47.4 ppm, representing 15% of the phosphorus products, to the carbonyl hydride complexes **4** and **5**, respectively. These compounds usually form by reaction of **2** with primary alcohols,<sup>17b</sup> but contamination during the methanol wash following the synthesis is unlikely to account for the 15% of hydride produced here. Indeed,  $^1\text{H}$  NMR only confirmed the presence of **4** and **5** (characteristic triplet at  $\delta$  -24.25 ppm and a doublet at  $\delta$  -24.95 ppm) as traces. Therefore, unknown phosphorus compounds must appear around the same shifts as the carbonyl compounds. As a matter of fact, no carbonyl stretch was observable by IR analysis (usually in the range 1890–1920  $\text{cm}^{-1}$ ). A third unidentified hydride is visible on the  $^1\text{H}$  NMR as a doublet at  $\delta$  -7.43 ppm ( $^2J = 50$  Hz) that had also been observed by reaction of **2** with primary alcohols.

(33) The decomposition is indicated by the steady disappearance of the carbene signal at  $\delta$  19.63 ppm.

**Table 1.** Selected Bond Lengths (Å) and Angles (deg) for Complexes **2** and **8**

	<b>2</b>	<b>8</b>
Bond Lengths		
Ru–C(1)	2.085(2)	2.076(3)
Ru–C(20)	1.835(2)	1.844(3)
Ru–Cl(1)	2.3988(5)	2.3644(9)
Ru–Cl(2)	2.3912(5)	2.4302(10)
Ru–P	2.4245(5)	2.4298(8)
Bond Angles		
C(20)–Ru–C(1)	100.24(8)	98.37(11)
C(1)–Ru–Cl(1)	94.55(5)	88.90(8)
C(1)–Ru–Cl(2)	83.26(5)	89.65(8)
C(20)–Ru–Cl(1)	89.14(7)	105.17(9)
C(20)–Ru–Cl(2)	103.15(7)	87.50(9)
Cl(1)–Ru–Cl(2)	167.71(2)	167.32(4)
C(1)–Ru–P	163.73(6)	163.29(7)
C(20)–Ru–P	95.89(6)	97.33(9)

Even though the  $^2\text{H}$  NMR does not indicate the presence of a ruthenium deuteride, a number of deuterated species have formed. Most signals overlap between 1 and 3 ppm, collapsing into a broad base, which accounts for the deuterated methyls of the NHC ligand of the different decomposed ruthenium complexes. The  $^{13}\text{C}$  NMR did not reflect the presence of any carbonyl compound or carbide. Since no compound could be isolated, we tested the isomerization behavior of this decomposition mixture on 1-octene using typical reaction conditions.<sup>11b,34</sup> No decomposition product of complex **8** was able to isomerize olefins to the extent observed with the original metathesis catalyst (5% of isomers were obtained here vs 76% obtained with catalyst **2** in similar conditions).<sup>11a</sup>

Because the methylidene is a key intermediate in most metathesis reactions, we also examined its decomposition in situ by reacting **8** with excess ethylene in benzene at 60 °C and stirring the mixture for 3 days.<sup>35</sup> Again, no sign of ruthenium

(34) In a previous report,<sup>11a</sup> we observed that, after 24 h at 55 °C, a 2.3 M solution of catalyst **2** in neat 1-octene afforded 76% isomers. In the present case, the catalytic mixture was dried under vacuum once fully decomposed (no more carbene signal on the  $^1\text{H}$  NMR), and 0.5 g of 1-octene was added. The reaction mixture was allowed to stand at 55 °C for 24 h, and the isomer content was determined by  $^1\text{H}$  NMR by integration of the internal olefin peak at  $\delta$  5.40 ppm.

(35) When the reaction mixture was sampled for  $^1\text{H}$  NMR, these conditions led to the complete transformation of benzylidene **8** into the methylidene, which decomposed rapidly, as indicated by the disappearance of the methylidene signal at 18.40 ppm.

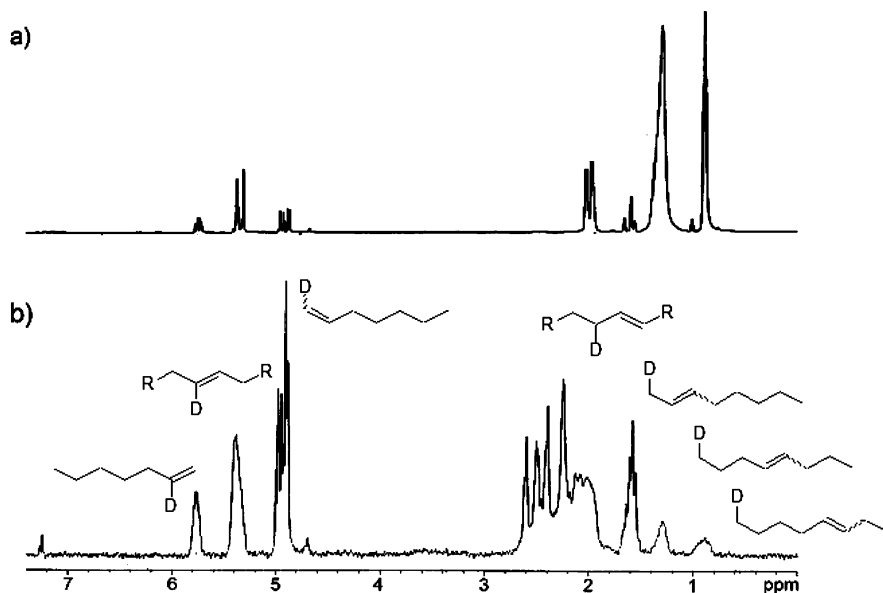


**Figure 11.** (a)  $^1\text{H}$  NMR and (b)  $^2\text{H}$  NMR spectrum of neat 1-octene with 0.5 mol % of complex **8**, after 4 h at 35 °C and 20 h at 55 °C.

deuteride was detectable by  $^2\text{H}$  NMR, and the same peaks, observed during the decomposition of the benzylidene, appeared between 1 and 3 ppm. Interestingly, a singlet at  $\delta$  7.14 ppm indicated the presence of partially deuterated benzene,<sup>36</sup> suggesting the existence of an H/D exchange process between ligand and solvent, since the only original source of deuterium in this case was the methyl groups of the carbene ligand methylidene of complex **8**. A similar exchange with solvent was observed for the ruthenium dihydride (IMes)Ru(H)<sub>2</sub>(H<sub>2</sub>)<sub>2</sub>PCy<sub>3</sub>,<sup>37</sup> and other dihydrides have been shown to undergo exchange processes.<sup>38</sup> The species responsible for this H/D exchange may also be a ruthenium dihydride, which may not be detectable because of NMR detection/concentration limits. Indeed, many hydride catalysts are too reactive to be observable spectroscopically under reaction conditions.

The catalytic mixture, once fully decomposed, was again tested for isomerization activity using 1-octene under the same conditions as used previously. Even though the isomerization extent was increased to 25% isomers, the decomposition products of complex **8**'s methylidene *alone* did not match the isomerization behavior observed with catalyst **2** under metathesis conditions, i.e., in the presence of an olefin, which suggests that the isomerization process involves more than simply decomposition products. Other intermediates of the metathesis cycle must play a role in the formation of the hydride responsible for this side reaction. For example, Forman et al. have described the decomposition of a metallacyclobutane through  $\beta$ -H abstraction to form a ruthenium hydride and explained the appearance of different alkenes from the metathesis of ethylene with [Ru]-**1**.<sup>39</sup>

Hence, we decided to further investigate hydride formation in the presence of olefinic substrates to reflect true metathesis conditions.

**Catalytic Behavior under Metathesis Conditions.** We reasoned that if there were formation of a ruthenium deuteride by metal insertion into one of the methyl bonds, inevitably there would be deuterium incorporation on the olefin, which should be easily detectable by NMR.

To avoid any solvent contamination and allow the detection of both catalyst and substrate on the NMR scale, the experiments were run in neat substrate, the only deuterium source being complex **8**. First, we used 1-octene as our substrate, since we have based previous isomerization studies on this model.<sup>11</sup> A 0.5 mol % solution of complex **8** in 1-octene was monitored by  $^1\text{H}$  and  $^2\text{H}$  NMR at 35 °C for 4 h. These reaction conditions will ensure significant amounts of both metathesis and isomerization.<sup>11</sup> The  $^1\text{H}$  and  $^2\text{H}$  spectra were systematically superimposed to match chemical shifts, since no internal standard was available. Because of the chemical simplicity of the substrate, the distinction between isomers and metathesis products is virtually impossible by standard  $^1\text{H}$  NMR. Still, we know that under the present conditions metathesis occurs much more quickly than the isomerization process.

Shortly after the experiment was started, an internal olefin signal appeared on the proton spectrum, marking the beginning of the metathesis process, while the deuterium spectrum only showed the two singlets from the catalyst deuterated methyl groups. However, after 4 h, several other peaks became visible in the  $^2\text{H}$  spectrum, confirming incorporation of deuterium at various positions of the olefin backbone. Figure 11 shows the  $^1\text{H}$  and  $^2\text{H}$  NMR spectra taken *after 24 h* of reaction. A multiplet corresponding to the terminal olefin suggests the formation of CHD=CH(CH<sub>2</sub>)<sub>5</sub>CH<sub>3</sub>. Two other vinyl signals at  $\delta$  5.75 and 5.38 ppm, though smaller, evidence deuterium incorporation at the C-2 position of 1-octene and on an internal double bond, probably from an isomer of either 1-octene or 7-tetradecene. These observations are consistent with the presence of a metal deuteride, which is further supported by the emergence of peaks in the allylic region (around  $\delta$  2.0 ppm) followed by peaks in the alkane region (at  $\delta$  1.30 and 0.90 ppm), supposing that the isomerization reaction progresses along the olefin backbone to produce 1-*d*-2-, 1-*d*-3-, and 1-*d*-4-octene and 8-*d*-3-, 8-*d*-2-, and 8-*d*-1-octene, for example (Figure 12). The formation of the metal alkyl may be fast relative to the decomplexation of the olefin; thus, the same molecule of substrate can undergo several

(36) The deuterium content observed here is much superior to the levels naturally found in benzene.

(37) Giunta, D.; Hölsher, M.; Lehmann, C. W.; Mynott, R.; Wirtz, C.; Leitner, W. *Adv. Synth. Catal.* **2003**, *345*, 1139–1145.

(38) (a) Burtling, S.; Mahon, M. F.; Paine, B. M.; Whittlesey, M. K.; Williams, J. M. J. *Organometallics* **2004**, *23*, 4537–4539. (b) Abdur-Rashid, K.; Fedorkiw, T.; Lough, A. J.; Morris, R. H. *Organometallics* **2004**, *23*, 86–94.

(39) van Rensburg, W. J.; Steynberg, P. J.; Meyer, W. H.; Kirk, M. M.; Forman, G. S. *J. Am. Chem. Soc.* **2004**, *126*, 14332–14333.

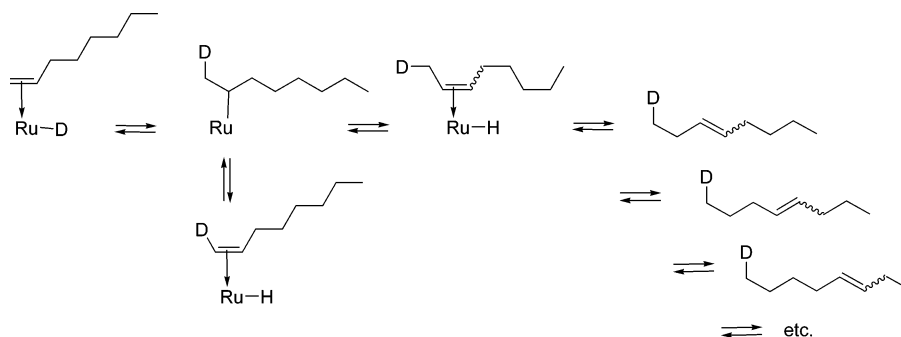


**Figure 12.** Formation of 1-octene isomers catalyzed by a ruthenium deuteride complex.

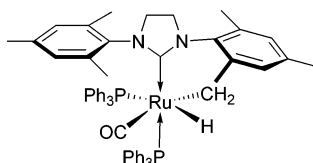


**Figure 13.** Complex **9**.

transformations before being released.<sup>13f</sup> Despite the large excess of 1-octene, it is also possible that some of the deuterated products come from isomerization of the metathesis product, although this cannot be quantified. It is worth noting that the alkyl deuterium signals are usually broader and flatter than those of their vinyl analogues because of multiple couplings. For this reason, the methyl signal expected for 1-*d*-2-octene at  $\delta$  1.60 ppm only becomes visible by <sup>2</sup>H NMR after longer reaction times. Nevertheless, deuterium atoms appear to preferentially incorporate at the C-1 position, suggesting a predominant Markovnikov addition of the metal deuteride across the double bond. When the temperature was raised to 55 °C, the concentration of these deuterated terminal olefins increased even more quickly. According to fundamental entropy thermodynamics, decomplexation of the olefin must occur to a greater extent at higher temperatures, therefore generating more olefins at a lower degree of isomerization. Indeed, after 20 h at 55 °C, the signal for the allylic methyl of 1-*d*-2-octene at 1.60 ppm has increased significantly and is now larger than other allylic or alkyl signals (Figure 11).

Aside from the signals of the deuterated methyl groups of the metathesis catalyst at  $\delta$  2.40 ppm, two broad singlets arise at 2.25 and 2.65 ppm. This indicates a transformation of the original complex. However, none of the complexes identified so far from catalyst decomposition could match our observations. Even though the multiple peaks between  $\delta$  2 and 3 ppm recall hydride complex **6** formed by thermal decomposition of the methylidene **2'**, they do not account for the formation of the metal deuteride evidenced in this experiment.<sup>20</sup> Likewise, we do not observe the characteristic signal from the Ru-CD<sub>2</sub>Ar moiety that would have probed the presence of 1 equiv of complex **7**. Of course, this does not exclude the possibility of a different C-D activation. In fact, hydride complex **9** shown in Figure 13, formed by insertion of ruthenium into the C-H bond of a mesityl group in the presence of alkenes, exhibits a broad "triplet" at 2.76 ppm from the protons of the Ru-CH<sub>2</sub>Ar moiety. Other examples of C-H activation from ruthenium carbenes could partially match these signals; however, these assignments must remain speculations as long as the components of the mixture are not isolated.

As a matter of fact, no ruthenium deuteride species was detected, even after longer reaction times. The complex responsible for the isomerization process probably reacts more quickly than the NMR time scale allows for detection, or its

concentration is simply too low. However, we reasoned that if there was indeed formation of a ruthenium deuteride complex in sufficient amounts, then for each deuterium atom incorporated onto a substrate molecule, the corresponding ruthenium hydride species would be produced, according to the metal hydride addition-elimination mechanism. Therefore, this hydride complex may be visible by <sup>1</sup>H NMR as the isomerization process, producing the D/H exchange, goes on. A doublet appeared at  $\delta$  -20.36 ppm with <sup>2</sup>J<sub>HP</sub> = 17.8 Hz, characteristic of a hydride situated trans to an empty coordination site and cis to a phosphine.<sup>17d</sup> The same signal had been observed during the decomposition of the methylidene, and interestingly, only the methylidene remains at this point, implying that all the catalyst has either been activated by the olefin or decomposed. However, the information collected thus far does not allow us to conclude whether this hydride complex is in fact responsible for olefin isomerization under metathesis conditions.

The same experiment was performed with allyl methyl ether, which was used to evaluate the isomerization mechanism. We thought that dealing with an irreversible isomerization reaction would facilitate product identification, being limited by NMR spectroscopy in our interpretation. Again, 0.5 mol % of catalyst was used to provide sufficient deuterium content for NMR detection.

After 4 h at 35 °C, about 30% of metathesis product had formed, with no isomerization product detectable in the <sup>1</sup>H NMR, the high concentration of ether favoring the bimolecular metathesis process over the unimolecular isomerization reaction. The <sup>2</sup>H NMR spectrum shows deuterium incorporation mostly at the terminal carbon of the olefin, as allyl-3-*d* methyl ether,<sup>40</sup> the signal matching perfectly the pattern of the <sup>1</sup>H spectrum (Figure 14). Deuterated ethylene is also present in significant amounts, more likely by metathesis of allyl-3-*d* methyl ether. Again, this is consistent with the presence of a metal deuteride complex. Smaller resonances at 1.68 ppm indicate the formation of isomerized product, as 3-*d*-1-methoxypropene.

Surprisingly, a triplet at 3.13 ppm and a doublet at 3.72 ppm suggest the presence of deuterons at the C-4 and C-1 positions of the starting material (less than 0.3%), respectively. A classical metal hydride mechanism cannot explain deuteration at these positions, nor can a  $\pi$ -allyl mechanism. Hence, an alternate mechanism must be proceeding competitively; however, to a much lower extent. The H/D exchange process observed during the decomposition of complex **8**'s methylidene may also be operating here. If this is the case, the introduction of a nonisomerizable olefin, such as 3,3-dimethylbutene, should result in the deuteration of every position and, more particularly, of the methyl groups.

(40) Due to the large excess of allyl methyl ether, we suppose that at early reaction times the molecules are only monodeuterated, since they are not likely to react again with another ruthenium deuteride.



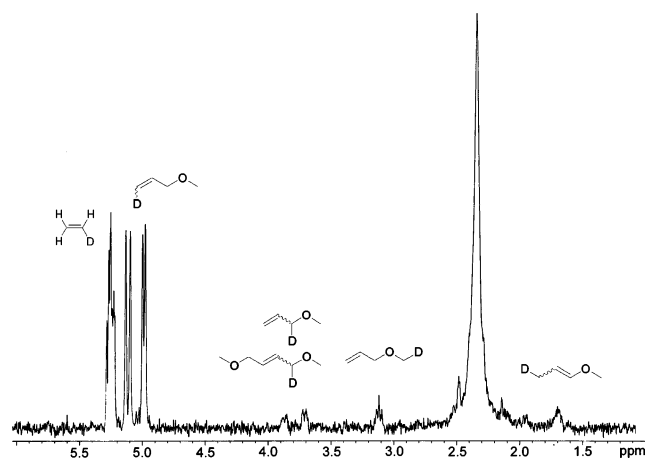


**Figure 14.**  $^2\text{H}$  NMR spectrum of neat allyl methyl ether with 0.5 mol % of complex **8**, after 4 h at 35 °C.

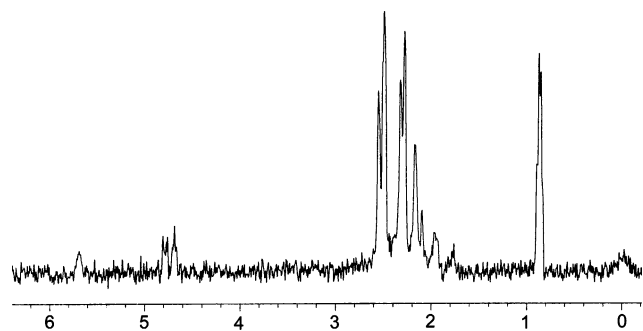


**Figure 15.**  $^2\text{H}$  NMR spectrum of neat 3,3-dimethylbutene with 0.5 mol % of complex **8**, after 4 h at 35 °C.

To look into this potential H/D exchange process, we repeated the experiment with 3,3-dimethylbutene for its inherent inability to isomerize. We reasoned that if there were indeed formation of a “classical” ruthenium deuteride, we would observe deuterium incorporation *exclusively* at the C-1 and C-2 positions. In addition, the metathesis reaction of olefins containing allylic methyls is known to proceed at a slow rate, if at all. In fact, the cross-metathesis of 3,3-dimethylbutene with **1** only resulted in an accumulation of the methylidene complex by nonproductive metathesis.<sup>41</sup> Accordingly, after 4 h at 35 °C, metathesis conversions merely reached 10%.

Figure 15 illustrates the corresponding  $^2\text{H}$  NMR. Even though there are signs of deuteration on the double bond (signals at  $\delta$  5.70 and 4.70 ppm), most displaced deuterons are on the methyl groups, as indicated by the major peak at 0.86 ppm. This is clearly the result of an H/D exchange process, although not necessarily direct, between the methyl groups of the NHC ligand and the C–H bond of the substrate. It is likely that the deuterium atoms are transferred to the metal center from the NHC methyl groups and then onto the substrate. Again, this type of transfer could very well be the result of ruthenium insertion into the methyl C–D bond, the cyclometalation of a substituent on a nitrogen-ligated carbene on ruthenium being a fairly common reaction, albeit not well understood.<sup>17d,21,38,42</sup> Interestingly, the ruthenium dihydride (IMes)Ru(H)<sub>2</sub>(H<sub>2</sub>)<sub>2</sub>PCy<sub>3</sub> promotes a similar exchange from the mesityl methyl groups to a variety of aromatic compounds, although preferentially exchanging with

$\text{sp}^2$  rather than  $\text{sp}^3$  C–H bonds.<sup>37</sup> Even though the event of the formation of a dihydride complex from a ruthenium carbene in the absence of dihydrogen may seem unlikely,<sup>15</sup> the reactivity of the phosphine-free methylidene offers many possibilities. For instance, Stradiotto *et al.* reported a reversible  $\alpha$ -H elimination allowing the interconversion of Ru=C and Ru–alkyl species.<sup>43</sup> The electrophilicity of the methylidene carbon also renders it highly sensitive to nucleophilic attack.<sup>44</sup> In fact, Grubbs *et al.* proposed that the first step toward formation of bimetallic complex **6** involves nucleophilic attack by free phosphine to form a ruthenium alkyl complex.<sup>20</sup> Certainly, the hypothesis of a ruthenium dihydride is not ruled out by the spectroscopy analysis of **2'** decomposition. One of the observed hydride signals may very well be one of a dihydride. Finally, the same dihydride complex could be responsible for both the exchange process and the isomerization reaction.

The rate of the H/D exchange process apparently depends on the substrate. Indeed, we observe greater deuterium incorporation on the methyls of 3,3-dimethylbutene than on allyl methyl ether. The extensive production of the methylidene complex, inherent to the metathesis of olefins containing allylic methyls, accelerates the rate of catalyst decomposition, which is probably in direct correlation with the formation of the species promoting the exchange process.

## Conclusions

A deuterium labeling study was undertaken to determine the mechanism of olefin isomerization during the metathesis reactions catalyzed by a second-generation Grubbs catalyst. The reaction of allyl-1,1- $d_2$  methyl ether with **2** at 35 °C was followed by  $^1\text{H}$  and  $^2\text{H}$  NMR spectroscopy. The evidence of deuterium incorporation at the C-2 position allowed us to conclude that a metal hydride addition–elimination mechanism was operating under these conditions. When the reaction was conducted in a closed system, the isomerization rate was calculated at approximately  $5.59 \times 10^{-6} \text{ s}^{-1}$ , while the equilibrium constant was about  $4.04 \times 10^{-6}$ .

The next step was an attempt to identify the eventual role of the NHC ligand in the formation of the hydride species responsible for the isomerization reaction. We synthesized complex **8**, an analogue of **2**, bearing deuterated *o*-methyl groups on the aromatic rings of the NHC ligand. Its decomposition afforded several metal hydride species; however, no deuteride complex was detected by  $^2\text{H}$  NMR spectroscopy. The methylidene analogue **8'** was also subjected to thermal decomposition but again did not afford any detectable ruthenium deuteride complex. The isomerization activities of the catalytic decomposition mixtures were tested with benchmark 1-octene but did not match the isomerization rates observed with **2** under similar metathesis conditions, proving that thermal decomposition products from this catalyst do not promote the isomerization reaction. Hence, other metathesis intermediates, such as the metallacyclobutane, must be involved in the isomerization process. Indeed, when complex **8** was reacted with 1-octene, a variety of deuterated olefins were produced, indicating the presence of a deuteride complex, albeit not observable spectroscopically. Finally, reaction of **8** with allyl methyl ether and 3,3-dimethylbutene actually revealed the existence of a competitive H/D exchange process between the CD<sub>3</sub> groups on the NHC ligand and the C–H bonds of the substrate. We propose that

(41) Ulman, M.; Grubbs, R. H. *Organometallics* **1998**, *17*, 2484–2489.

(42) (a) Owen, M. A.; Pye, P. L.; Piggott, B.; Capparelli, M. V. *J. Organomet. Chem.* **1992**, *434*, 351–362. (b) Hitchcock, P. B.; Lappert, M. F.; Pye, P. L.; Thomas, S. *J. Chem. Soc., Dalton Trans.* **1979**, *88*, 1929–1942.

(43) Rankin, M. A.; McDonald, R.; Ferguson, M. J.; Stradiotto, M. *Angew. Chem., Int. Ed.* **2005**, *44*, 3603–3606.

(44) Hansen, S. M.; Rominger, F.; Metz, M.; Hofmann, P. *Chem. Eur. J.* **1999**, *5*, 557–566.

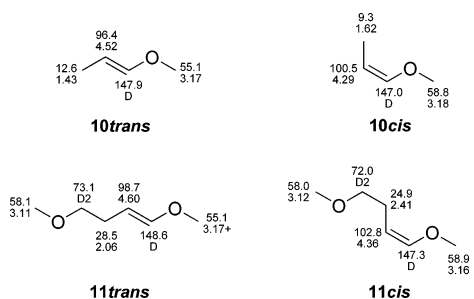


**Figure 16.**  $^1\text{H}$  and  $^{13}\text{C}$  chemical shift assignments in the compounds **10cis**, **10trans**, **11cis**, and **11trans**.

the H/D exchange is promoted by a ruthenium dihydride intermediate whose formation is closely related to the methylenide decomposition. Further studies must be conducted to isolate and characterize these hydride complexes. Meanwhile, hydride traps should be used during metathesis reactions catalyzed by ruthenium carbenes in order to prevent competitive isomerization.<sup>45</sup>

## Experimental Section

**General Considerations.** Routine  $^1\text{H}$  NMR (300 MHz) and  $^{13}\text{C}$  NMR (75 MHz) measurements were recorded on either a Mercury Series or Varian VXR-300 NMR superconducting spectrometer. Chemical shifts are reported in ppm relative to tetramethylsilane (TMS) or residual proton from the solvent. All organometallic spectra were recorded in  $d_6$ -benzene, previously dried over Na/K alloy and degassed by three freeze–pump–thaw cycles.

All materials were purchased from Aldrich and used as received, except for the THF and ether that were previously dried over a catalyst bed. Complex **2**,<sup>46</sup> allyl-1,1- $d_2$  methyl ether,<sup>47</sup> and (trimethylsilyl)methyl azide (TMSMA)<sup>48</sup> were synthesized according to the literature. Allyl-1,1- $d_2$  methyl ether was distilled, degassed by three freeze–pump–thaw cycles, and stored in a glovebox.

**Deuterium Labeling Study with Allyl-1,1- $d_2$  Methyl Ether.** In the drybox, 4 mg (0.005 mmol) of complex **2** was dissolved with 0.8 mL of  $\text{C}_6\text{D}_6$  or toluene- $d_8$  in a J. Young valve NMR tube, and this solution was then layered with 185 mg (2.5 mmol) of allyl-1,1- $d_2$  methyl ether. The tube was shaken right before being loaded into the NMR instrument.

NMR spectra were recorded on a Varian Inova spectrometer equipped with a 5 mm indirect detection probe, operating at 500 MHz for  $^1\text{H}$  and at 125 MHz for  $^{13}\text{C}$ . The temperature was 35 °C. Chemical shifts are reported in ppm relative to TMS. The residual methyl signal of the solvent was used as reference (2.09 ppm for  $^1\text{H}$  and 20.4 ppm for  $^{13}\text{C}$ ).

The sample is a mixture of four compounds, **10cis**, **10trans**, **11cis**, and **11trans**, shown in Figure 16. Each of these compounds is a mixture of the four isotopomers resulting from partial deuteration in positions 2 and 3 of the alkylene ether. Positions 1 and 4 are completely deuterated. The relative ratios of the four compounds and the molar fractions of deuteration in each position are given in Figure 17.

The proton spectrum displays in the region 4.70–4.20 ppm the signals of a mixture of four compounds (Figure 18): quartets for the compounds **10cis** and **10trans** and triplets for the compounds

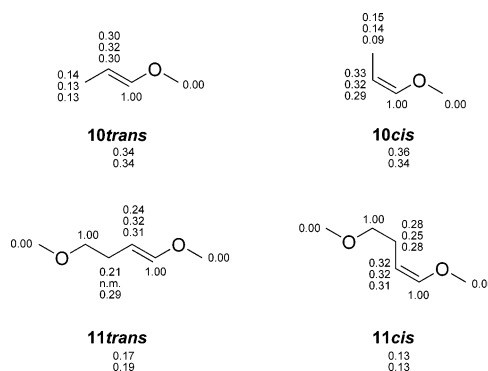


**Figure 17.** Molar fractions of compounds **10cis**, **10trans**, **11cis**, and **11trans** in the product (under the compound number) and molar fractions of deuteration at each position. The number on top was based on the proton spectrum and the second number on the deuterium spectrum. The number on the bottom for the molar fraction of deuteration was based on the integral of the proton signal at that position and the composition determined in the deuterium spectrum, and it is the most reliable.

**11cis** and **11trans**. All of these signals display an extra coupling with deuterium: triplet in a 1:1:1 ratio.

These signals present in the gHMBC spectrum (Figure 19) a one-bond coupling to a carbon in the range 96–102 ppm and two long-range couplings, one with a carbon at 9–28 ppm and one with a carbon at 147–149 ppm. This latter carbon displays a triplet in f1, consistent with a one-bond coupling with deuterium, and also a long-range coupling to protons at 3.16–3.18 ppm, protons which are on carbons at 55–60 ppm. The protons on the carbons at 9–28 ppm are in the range 1.43–2.41 ppm and couple with both the carbons at 96–102 ppm and with the carbons at 147–149 ppm. These proton–carbon couplings, together with the characteristic chemical shifts, identify the methyl-1-propenyl ether fragment in all four compounds. In the compounds **11cis** and **11trans**, the aliphatic protons at 2.06 and 2.41 ppm couple with carbons at 73.1 and 72.0 ppm, respectively. Both of these carbons carry no protons and couple with the protons of a methoxy group. The NOESY spectrum reveals NOE's between the alkene proton and the methoxy protons of the methyl vinyl ether fragment in compounds **10trans** and **11trans** only; therefore, in these compounds the double bond is *E*. In these compounds the proton–deuterium coupling across the double bond is ca. 1.8 Hz, while in the *Z* compounds **10cis** and **11cis**, it is ca. 0.9 Hz.

The carbon spectrum (Figure 20) confirms the lack of deuterium on the methoxy groups and complete deuteration at position 1 of the alkene fragment, for all four compounds. In compounds **11cis** and **11trans**, the signals at 73.1 and 72.0 ppm could barely be seen, as broad multiplets, confirming that these carbons carry only deuterium. With two positions with partial deuteration, compounds **10cis**, **10trans**, **11cis**, and **11trans** are each present as four isotopomers. This is why the carbons in position 3 of the alkene fragments display a pattern of eight lines—the one at higher field is the H<sub>3</sub>H<sub>2</sub> isotopomer, followed by the line of the H<sub>3</sub>D<sub>2</sub> isotopomer. The next six lines are less intense and belong to the triplets of the D<sub>3</sub>H<sub>2</sub> and D<sub>3</sub>D<sub>2</sub> isotopomers. The carbon chemical shifts in Figure 16 are those of the H<sub>2</sub>H<sub>3</sub> isotopomer.

The molar fractions of the four compounds in the mixture and the fractions of deuterium substitution at each position were determined by integration of the signals in both the proton and the deuterium spectra. They are given in Figure 17, as the first and second sets of values, respectively. The spectra were taken at 70 °C, when the separation of the signals of interest was optimal. In the proton spectrum, the signals of the methoxy groups were used, since there is no deuteration of these groups. Four signals could be integrated separately: 3.22–3.20 (**10cis**), 3.20–3.18 (**10trans** + **11cis** + **11trans**), 3.14–3.12 (**11cis**), and 3.12–3.11 ppm (**11trans**).

(45) A recent paper shows the use of benzoquinone to prevent olefin isomerization during metathesis reactions: Hong, S. H.; Sanders, D. P.; Lee, C. W.; Grubbs, R. H. *J. Am. Chem. Soc.* **2005**, *127*, 17160–17161.

(46) Scholl, M.; Ding, S.; Lee, C.; Grubbs, R. H. *Org. Lett.* **1999**, *1*, 953–956.

(47) McGrath, D. V.; Grubbs, R. H. *Organometallics* **1994**, *13*, 224–235.

(48) Nishiyama, K.; Tanaka, N. *J. Chem. Soc., Chem. Commun.* **1983**, 22, 1322–1323.

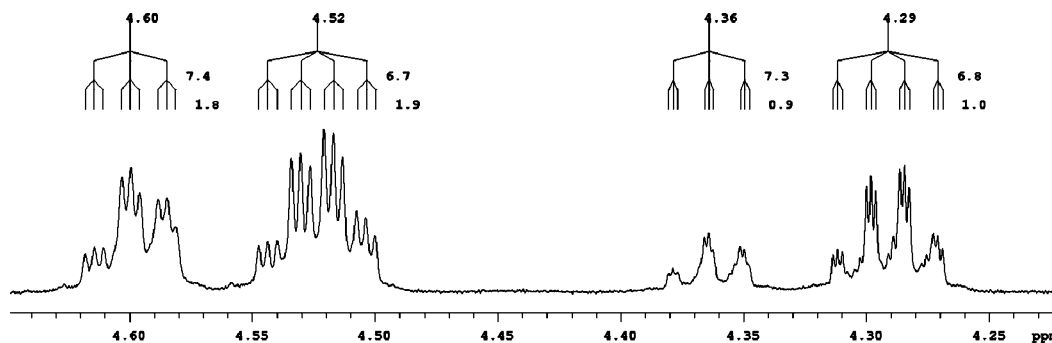


Figure 18. Expansion of the proton spectrum, the CH<sub>2</sub> region.

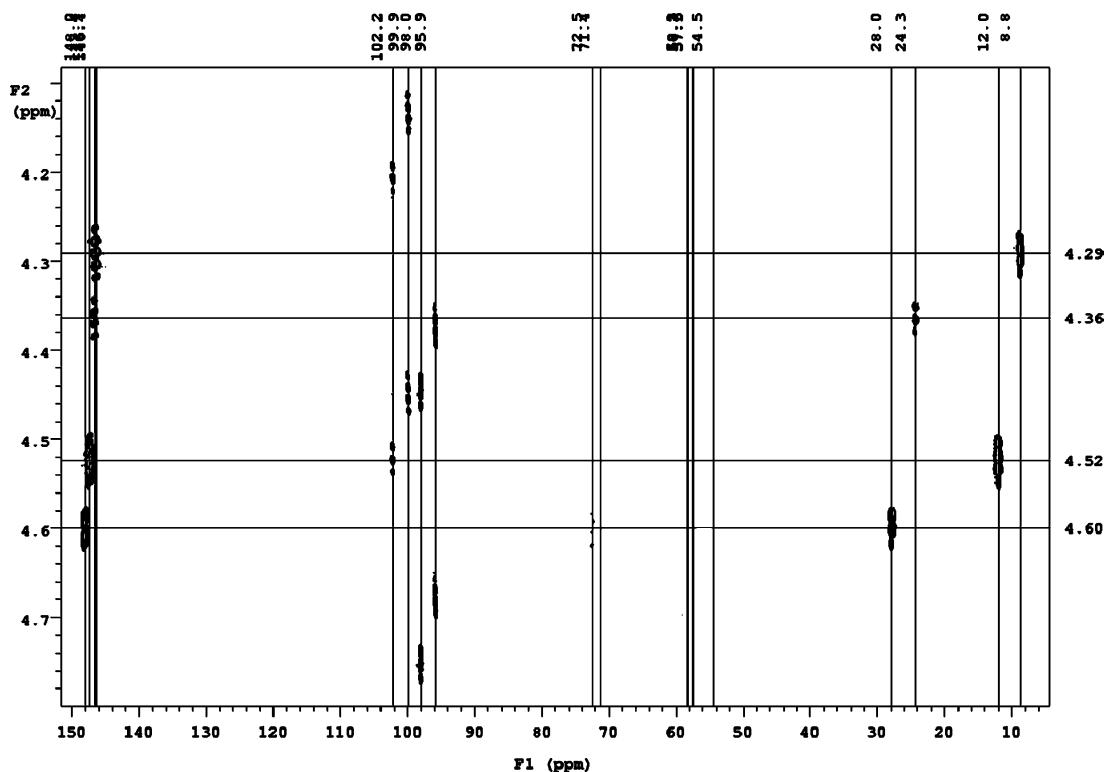


Figure 19. Expansion of the gHMBC spectrum.

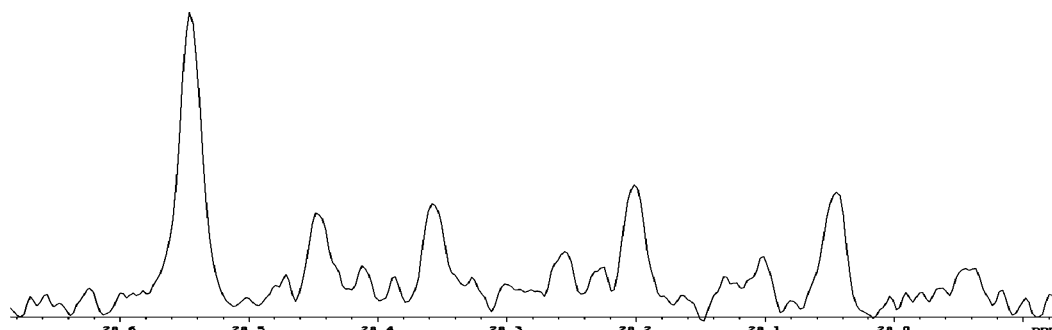


Figure 20. Expansion of the carbon spectrum, C3 region.

The separation of the last two signals is marginal, and for this reason the values for the relative ratio of the four compounds determined in the proton spectrum are considered to be less precise than the values determined in the deuterium spectrum. Four signals in the deuterium spectrum were used: 6.30–6.12 (position 1 in **10trans** + **11trans**), 5.78–5.62 (position 1 in **10cis** + **11cis**), 3.30–3.20 (position 3 in **11cis**), and 3.20–3.09 ppm (position 3 in **11trans**).

The fraction of deuteration at positions 2 and 3 was determined in both the proton and the deuterium spectra. The separation of the signals was poorer in the deuterium spectrum, in which also the signal of position 3 in **11trans** was overlapping the methyl signal

of toluene. We consider that the best approach is to determine the relative ratios of compounds in the deuterium spectrum and then to use these ratios and the integrals from the proton spectrum to calculate the fraction of deuteration at each position. Values determined this way are presented in the third row in Figure 17.

**Deuterium Labeling Study with Allyl-1,1-*d*<sub>2</sub> Methyl Ether.** In the drybox, 4 mg (0.005 mmol) of complex **2** was dissolved with 0.8 mL of C<sub>6</sub>D<sub>6</sub> in a J. Young valve NMR tube, and this solution was then layered with 185 mg (2.5 mmol) of allyl-1,1-*d*<sub>2</sub> methyl ether. The tube was shaken right before being loaded in the NMR instrument. The reaction was monitored by <sup>1</sup>H NMR at

35 °C, and the conversions were calculated by integration of the peaks at  $\delta$  4.98 and 5.72 ppm for the starting material and metathesis product, respectively, against the solvent residual peak, every 120 s.

**X-ray Studies.** Experimental data:  $C_{40}H_{61}Cl_2N_2PRu$ ,  $M_r = 820.9$ , triclinic,  $P\bar{1}$ ,  $a = 11.706(18)$  Å,  $b = 12.316(19)$  Å,  $c = 16.042(3)$  Å,  $\alpha = 87.77(3)^\circ$ ,  $\beta = 70.83(2)^\circ$ ,  $\gamma = 70.93(3)^\circ$ ,  $V = 2058.5(6)$  Å<sup>3</sup>,  $Z = 2$ ,  $D_{\text{calcd}} = 1.32$  g cm<sup>-3</sup>, Mo K $\alpha$  radiation ( $\lambda = 0.710$  73 Å),  $T = 173$  K.

Data were collected at 173 K on a Siemens SMART PLAT-FORM equipped with a CCD area detector and a graphite monochromator utilizing Mo K $\alpha$  radiation ( $\lambda = 0.710$  73 Å). Cell parameters were refined using up to 8192 reflections. A full sphere of data (1850 frames) was collected using the  $\omega$ -scan method (0.3° frame width). The first 50 frames were remeasured at the end of data collection to monitor instrument and crystal stability (maximum correction on  $I$  was <1%). Absorption corrections by integration were applied on the basis of measured indexed crystal faces.

The structure was solved by direct methods in SHELXTL6 and refined using full-matrix least squares. The non-H atoms were treated anisotropically, whereas the hydrogen atoms were calculated in ideal positions and were riding on their respective carbon atoms. The structure has two disorders. The first disorder is a minor one where the C2–C3 moiety is refined in two parts with their site occupation factors independently refined. The second disorder is a major one involving the triphenylphosphine group and the C20 ligand according to a pseudo-mirror symmetry passing through Ru and C1 and bisecting the C2–C3 bond. A total of 539 parameters were refined in the final cycle of refinement using 13 498 reflections with  $I > 2\sigma(I)$  to yield R1 and wR2 values of 3.77% and 8.40%, respectively. Refinement was done using  $F^2$ .<sup>49</sup>

**Synthesis of Complex 8. (a) Synthesis of 2-Bromoisophthalic Acid (B).** In a round-bottom flask equipped with a condenser, 25.0 g of bromoxylene (0.135 mol) was dissolved in 200 mL of 1:1 <sup>t</sup>BuOH–water. Two equivalents of KMnO<sub>4</sub> (42.7 g, 0.270 mol) was added portionwise, and the solution was refluxed for 4 h. After the mixture was cooled, 2 equiv more of KMnO<sub>4</sub> was added, and the solution was refluxed overnight. The mixture was filtered through a Celite bed while still hot, and the filtrate was concentrated to one-third of its original volume. Concentrated H<sub>2</sub>SO<sub>4</sub> was added slowly until a white precipitate formed. Filtration and drying under vacuum afforded 32.7 g (0.133 mol, 99%) of a white powder (mp >250 °C). <sup>1</sup>H NMR (CD<sub>3</sub>OD, 300 MHz):  $\delta$  7.73 (d, 2H, *meta* CH, <sup>2</sup>J<sub>H,H</sub> = 7.6 Hz), 7.48 (t, 1H, *para* CH, <sup>3</sup>J<sub>H,H</sub> = 7.8 Hz), 5.32 (s, 2H, COOH). <sup>13</sup>C NMR (CD<sub>3</sub>OD, 75 MHz):  $\delta$  = 169.9, 137.7, 138.5, 128.4, 118.3. LRMS/EI: calcd for C<sub>8</sub>H<sub>5</sub>BrO<sub>4</sub>,  $m/z$  245; found,  $m/z$  245.

**(b) Synthesis of Dimethyl 2-Bromoisophthalate.** 2-Bromoisophthalic acid (32.7 g, 0.133 mol) was dissolved in DMF. Two equivalents (37.0 g, 0.270 mol) of K<sub>2</sub>CO<sub>3</sub> and 38.0 g (0.27 mol, 2.0 equiv) of methyl iodide were added to the solution, as well as a catalytic amount of CeCO<sub>3</sub>. The reaction mixture was stirred overnight at room temperature and quenched with acidic water until all the base dissolved. The aqueous solution was extracted with ether. Afterward the organic layer was washed with water, dried over MgSO<sub>4</sub>, and concentrated to a yellow oil (30.0 g, 0.110 mol, 81%). <sup>1</sup>H NMR (CDCl<sub>3</sub>, 300 MHz):  $\delta$  7.68 (d, 2H, *meta* CH, <sup>2</sup>J<sub>H,H</sub> = 7.4 Hz), 7.40 (t, 1H, *para* CH, <sup>3</sup>J<sub>H,H</sub> = 7.8 Hz), 3.94 (s, 3H, COOCH<sub>3</sub>). <sup>13</sup>C NMR (CDCl<sub>3</sub>, 75 MHz):  $\delta$  166.6, 135.2, 132.1, 127.1, 118.7, 52.6. MS (LRMS/EI): calcd for C<sub>10</sub>H<sub>9</sub>BrO<sub>4</sub>,  $m/z$  273; found,  $m/z$  273.

**(c) Synthesis of 2-Bromo-1,3-bis(hydroxy-*d*<sub>2</sub>-methyl)benzene (C).** In a flame-dried round-bottom flask immersed in an ice bath, 9.23 g (0.219, 2.0 equiv) of lithium aluminum deuteride was suspended in 200 mL of dry THF. Dimethyl 2-bromoisophthalate (30.0 g, 0.110 mol) diluted in 20 mL of dry THF was added

dropwise at 0 °C. After the addition was complete, the slurry was stirred for 20 min. The reaction mixture was quenched and worked up following the standard procedure,<sup>50</sup> to yield 20.6 g (0.093 mol, 85%) of a white powder (mp 152–154 °C). <sup>1</sup>H NMR (pyridine-*d*<sub>5</sub>, 300 MHz):  $\delta$  7.95 (d, 2H, *meta* CH, <sup>2</sup>J<sub>H,H</sub> = 7.2 Hz), 7.50 (t, 1H, *para* CH, <sup>3</sup>J<sub>H,H</sub> = 7.5 Hz), 5.14 (s, 2H, OH). <sup>13</sup>C NMR (pyridine-*d*<sub>5</sub>, 75 MHz):  $\delta$  140.9, 126.3, 125.6, 112.1, 62.2 (q, CD<sub>2</sub>OH); MS (LRMS/EI): calcd for C<sub>8</sub>H<sub>5</sub>D<sub>4</sub>BrO<sub>2</sub>,  $m/z$  221, found,  $m/z$  221.

**(d) Synthesis of 2-Bromo- $\alpha,\alpha'$ -dibromo-*m*-xylene-*d*<sub>4</sub>.** 2-Bromo-1,3-bis(hydroxy-*d*<sub>2</sub>-methyl)benzene (20.6 g, 0.093 mol) was suspended in a solution of CBr<sub>4</sub> (71.2 g, 0.214 mol, 2.3 equiv) in dichloromethane. Triphenylphosphine (57.4 g, 0.219 mol, 2.35 equiv) was added portionwise at room temperature to avoid overheating. After the addition was complete, the clear solution was precipitated in ether and filtered. As the solvent was evaporated, any remaining triphenylphosphine was further filtered. The crude product was purified via column chromatography using 5:1 hexanes–ethyl acetate to yield 22.5 g (0.065 mol, 70%) of a white powder (mp 85–88 °C). <sup>1</sup>H NMR (CDCl<sub>3</sub>, 300 MHz):  $\delta$  7.41 (d, 2H, *meta* CH, <sup>2</sup>J<sub>H,H</sub> = 7.3 Hz), 7.28 (t, 1H, *para* CH, <sup>3</sup>J<sub>H,H</sub> = 7.2 Hz). <sup>13</sup>C NMR (CDCl<sub>3</sub>, 75 MHz):  $\delta$  138.4, 128.4, 127.9, 126.9, 33.9 (q, CD<sub>2</sub>Br, <sup>5</sup>J<sub>C,D</sub> = 18.9 Hz); MS (LRMS/EI): C<sub>8</sub>H<sub>3</sub>D<sub>4</sub>Br<sub>3</sub> = 347, found 347.

**(e) Synthesis of 2-Bromo-*m*-xylene-*d*<sub>6</sub> (D).** In a flame-dried flask, 2-bromo- $\alpha,\alpha'$ -dibromo-*m*-xylene-*d*<sub>4</sub> (22.5 g, 0.065 mol) in THF was added dropwise to a slurry of lithium aluminum deuteride (2.73, 0.065 mol) in dry THF at room temperature. Then, the reaction mixture was quenched and worked up following the standard procedure,<sup>50</sup> to yield 11.2 g (0.058 mol, 90%) of a colorless liquid. <sup>1</sup>H NMR (CDCl<sub>3</sub>, 300 MHz):  $\delta$  7.05 (m, 3 Hz). <sup>13</sup>C NMR (CDCl<sub>3</sub>, 75 MHz):  $\delta$  138.4, 128.3, 127.8, 126.7, 23.2 (q, CD<sub>2</sub>Br, <sup>5</sup>J<sub>C,D</sub> = 18.8 Hz). MS (LRMS/EI): calcd for C<sub>8</sub>H<sub>3</sub>D<sub>6</sub>Br,  $m/z$  191; found,  $m/z$  191.

**(f) Synthesis of 2,6-dimethyl-*d*<sub>3</sub>-aniline (E).** In a flame-dried three-neck round-bottom flask equipped with a condenser, 11.2 g (0.058 mol) of 2-bromo-*m*-xylene-*d*<sub>6</sub> was added dropwise to a mixture of 1.71 g (0.070 mol, 1.2 equiv) of magnesium in 50 mL of anhydrous ether or a minimum amount. The solution was refluxed upon addition and was subsequently maintained at reflux for 2 h. After the reaction mixture was cooled to room temperature, a 1.2 M solution of TMSMA in ether was dripped into it, and this mixture was then stirred at room temperature for an additional 3 h. Water was added to quench the reaction mixture, and the ethereal phase was extracted, washed with brine, and dried over MgSO<sub>4</sub>. The crude product was purified through column chromatography in CH<sub>2</sub>Cl<sub>2</sub> to afford 4.09 g (0.032 mol, 55%) of an orange-yellow liquid. <sup>1</sup>H NMR (CDCl<sub>3</sub>, 300 MHz):  $\delta$  = 7.45 (d, 2H, *meta* CH, <sup>2</sup>J<sub>H,H</sub> = 7.8 Hz), 7.19 (t, 1H, *para* CH, <sup>3</sup>J<sub>H,H</sub> = 7.5 Hz), 4.46 (s, 2H, NH<sub>2</sub>); <sup>13</sup>C NMR (CDCl<sub>3</sub>, 75 MHz):  $\delta$  = 142.8, 128.4, 121.7, 118.2, 17.4 (q, CD<sub>3</sub>, <sup>5</sup>J<sub>C,D</sub> = 18.8 Hz); MS (LRMS/EI): calcd for C<sub>8</sub>H<sub>5</sub>D<sub>3</sub>N,  $m/z$  127; found,  $m/z$  127.

**(g) Synthesis of Glyoxalbis(2,6-dimethyl-*d*<sub>3</sub>-phenyl)imine.** The procedure was modified from the literature.<sup>51</sup> Under argon, a mixture of 2.12 g (0.014 mol) of a 40% aqueous solution of glyoxal, 2.3 mL of *n*-propanol, and 5.8 mL of water was combined with 4.09 g (0.032 mol, 2.2 equiv) of 2,6-dimethyl-*d*<sub>3</sub>-aniline in 20 mL of *n*-propanol. The solution was stirred at room temperature for 4 h and then at 60 °C for 2 h. Upon addition of 30 mL of water, a yellow solid precipitated. The mixture was chilled in ice to allow further precipitation, and 3.09 g (0.011 mol, 80%) was collected by filtration (mp 145–146 °C). <sup>1</sup>H NMR (CDCl<sub>3</sub>, 300 MHz):  $\delta$  8.13 (s, 2H, CH=N), 7.12 (d, 4H, *meta* CH, <sup>2</sup>J<sub>H,H</sub> = 7.4 Hz), 6.98

(50) Fieser, L. F.; Fieser, M. *Reagents for Organic Synthesis*; Wiley: New York, 1967; Vol. 1, pp 581–585.

(51) Arduengo, A. J., III; Krafczyk, R.; Schmutzler, R.; Craig, H. A.; Goerlich, J. R.; Marshall, W. J.; Unverzagt, M. *Tetrahedron* **1999**, *55*, 14523–14534.

(t, 2H, *para* CH,  $^3J_{\text{H,H}} = 7.7$  Hz).  $^{13}\text{C}$  NMR ( $\text{CDCl}_3$ , 75 MHz):  $\delta$  163.7, 150.1, 128.5, 126.5, 125.0, 17.4 (q,  $\text{CD}_3$ ,  $^5J_{\text{C,D}} = 18.9$  Hz). MS (HRMS/EI): calcd for  $\text{C}_{18}\text{H}_8\text{D}_{12}\text{N}_2$  [M + Na] $^+$ ,  $m/z$  299.2272; found,  $m/z$  299.2282.

**(h) Synthesis of Bis((2,6-dimethyl-*d*<sub>3</sub>-phenyl)amino)ethane Dihydrochloride.** A suspension of 3.09 g (0.011 mol) of the glyoxalbis(2,6-dimethyl-*d*<sub>3</sub>-phenyl)imine in 45 mL of 2:1 THF–methanol was treated with 1.70 g (0.044 mol, 4.0 equiv) of sodium borohydride at room temperature. The mixture was stirred for 16 h at room temperature and refluxed for 1 h. Upon cooling, 45 mL of ice–water was added, followed by 45 mL of 3 M hydrochloric acid. A white solid precipitated, which was filtered and washed with ether and acetone. Yield: 3.35 g (9.9 mmol, 85%); mp >250 °C.  $^1\text{H}$  NMR ( $\text{DMSO-}d_6$ , 300 MHz):  $\delta$  7.12 (s, 6H, *para*, *meta* CH), 3.60 (s, 4H,  $\text{NCH}_2$ ).  $^{13}\text{C}$  NMR ( $\text{DMSO-}d_6$ , 75 MHz):  $\delta$  135.5, 131.7, 129.9, 127.9, 17.8 (q,  $\text{CD}_3$ ,  $^5J_{\text{C,D}} = 18.8$  Hz). MS (LRMS/EI): calcd for  $\text{C}_{18}\text{H}_{14}\text{D}_6\text{N}_2\text{Cl}_2$ ,  $m/z$  352; found,  $m/z$  352.

**(i) Synthesis of 1,3-Bis((2,6-dimethyl-*d*<sub>3</sub>-phenyl)imidazolium Chloride (F).** A mixture of 3.35 g (9.9 mmol) of bis((2,6-dimethyl-*d*<sub>3</sub>-phenyl)amino)ethane dihydrochloride, 40 mL of triethyl orthoformate, and 2 drops of 96% formic acid was heated in a distillation apparatus until the distillation of ethanol ceased. Once the temperature rose toward 130 °C, the heating was stopped and the reaction mixture was cooled to room temperature. At this point, a white solid precipitated, which was isolated by vacuum filtration. Recrystallization from 2:1  $\text{CH}_3\text{CN}$ –ethanol afforded 1.67 g (5.7 mmol, 58%) of white crystals.  $^1\text{H}$  NMR ( $\text{CD}_3\text{CN}$ , 300 MHz):  $\delta$  9.38 (s, 1H,  $\text{NCHN}$ ), 7.32 (t, 2H, *para* CH,  $^3J_{\text{H,H}} = 7.7$  Hz), 7.24 (d, 4H, *meta* CH,  $^2J_{\text{H,H}} = 7.4$  Hz), 4.44 (s, 4H,  $\text{NCH}_2$ ).  $^{13}\text{C}$  NMR ( $\text{CD}_3\text{CN}$ , 75 MHz):  $\delta$  161.3, 137.0, 131.3, 130.1, 118.4, 52.1, 17.4 (q,  $\text{CD}_3$ ,  $^5J_{\text{C,D}} = 19.0$  Hz). MS (HRMS/EI): calcd for  $\text{C}_{19}\text{H}_{11}\text{D}_6\text{N}_2\text{Cl}$  [M] $^+$ ,  $m/z$  291.2609; found,  $m/z$  291.2621.

**(j) Synthesis of 1,3-Bis((2,6-dimethyl-*d*<sub>3</sub>-phenyl)-2-(trichloromethyl)imidazolidine (G).** To a solution of chlorine salt E (1.67 g, 5.7 mmol) in dry chloroform was added 0.230 g (5.7 mmol) of a 60% dispersion of sodium hydride. The reaction mixture was stirred at room temperature for 2 h and subsequently filtered. The filtrate was evaporated into a yellowish solid, which was flushed through a silica plug with 9:1 hexane–ethyl acetate. The ligand was further purified by recrystallization in boiling hexane, affording 3.28 g (4.7 mmol, 82%) of a white solid (mp 118–120 °C).  $^1\text{H}$  NMR ( $\text{CDCl}_3$ , 300 MHz):  $\delta$  7.03 (m, 6H, *para*, *meta* CH), 5.66 (s, 1H,  $\text{CHCCl}_3$ ), 3.98 (m, 2H,  $\text{NCH}_2$ ), 3.37 (m, 2H,  $\text{NCH}_2$ ).  $^{13}\text{C}$  NMR ( $\text{CDCl}_3$ , 75 MHz):  $\delta$  144.1, 138.4, 134.2, 129.5, 129.3, 125.6, 107.9, 86.1, 51.8, 19.0 (q,  $\text{CD}_3$ ,  $^5J_{\text{C,D}} = 19.0$  Hz). MS (HRMS/EI): calcd for  $\text{C}_{19}\text{H}_{10}\text{D}_{12}\text{N}_2$  [M + H] $^+$ ,  $m/z$  291.2609; found,  $m/z$  291.2622.

**(k) Synthesis of Complex 8.** The procedure was adapted from the literature.<sup>52</sup> In the drybox, a flame-dried Schlenk flask was charged with 0.879 g (1.07 mmol) of catalyst [Ru]1 and 1.640 g

(2.35 mmol, 2.2 eq) of ligand G. The mixture was dissolved in 25 mL of toluene and stirred at 60 °C for 90 min under argon. The solvent was then evaporated, and the brown residue was washed with methanol (2 × 25 mL) and pentane (50 mL). Finally, the pink solid was dried under vacuum to yield 0.693 g (0.83 mmol, 78%) of complex 8.  $^1\text{H}$  NMR (toluene-*d*<sub>8</sub>, 300 MHz):  $\delta$  19.57 (s, 1H, Ru=CH), 7.17 (t, 2H, *para* CH,  $^3J_{\text{H,H}} = 7.2$  Hz), 7.13–6.94 (m, 9H, *para*, *meta* CH), 6.54 (t, 1H,  $^3J_{\text{H,H}} = 7.3$  Hz), 3.43–3.15 (m, 4H,  $\text{NCH}_2\text{CH}_2\text{N}$ ), 2.41 (q, 3H), 1.55 (m, 15H), 1.08 (m, 15H).  $^{13}\text{C}$  NMR (toluene-*d*<sub>8</sub>, 75 MHz):  $\delta$  147.8, 129.5, 128.9, 128.6, 127.9, 125.8, 125.1, 32.4, 32.2, 30.3, 28.6, 28.5, 27.0, 20.8 (q,  $\text{CD}_3$ ,  $^5J_{\text{C,D}} = 19.7$  Hz).  $^{31}\text{P}$  NMR (toluene-*d*<sub>8</sub>, 300 MHz):  $\delta$  29.69. MS (HRMS/EI): calcd for  $\text{C}_{44}\text{H}_{48}\text{D}_{12}\text{N}_2\text{Cl}_2\text{PRu}$  [M] $^+$ ,  $m/z$  831.3656; found,  $m/z$  831.3648. Anal. Calcd for  $\text{C}_{44}\text{H}_{48}\text{D}_{12}\text{N}_2\text{Cl}_2\text{PRu}$ : C, 64.38; H, 7.49; N, 3.41. Found: C, 64.80; H, 7.39; N, 3.31.

**Thermal Decomposition of Complex 8.** In the drybox, 32 mg (0.038 mmol) of complex 8 was dissolved with 0.8 mL of  $\text{C}_6\text{D}_6$  in a glass ampule, which was then equipped with a Swedgelock connected to a Teflon Schlenk valve. The system was taken out of the glovebox, and the ampule was sealed under argon. The ampule was left in a 70 °C bath for 21 days and shaken regularly. It was then taken back into the drybox and transferred into a J. Young valve NMR tube.

**Thermal Decomposition of Methylidene Complex 8'.** In the drybox, a Schlenk tube was charged with 200 mg (0.038 mmol) of complex 8 dissolved in 10 mL of degassed benzene. The tube was taken out of the glovebox, connected to argon, and immersed in a 60 °C oil bath. Ethylene gas was bubbled rapidly through the solution for 30 min, resulting in a color change from pink to dark brown. The mixture was sampled to confirm full conversion of the benzyldiene by  $^1\text{H}$  NMR.

The mixture was then stirred at 60 °C for 3 days, after which the solvent was evaporated in vacuo. The flask was taken back into the drybox and transferred into a J. Young valve NMR tube.

**Isomerization Experiment.** Once no more carbene signal was visible by  $^1\text{H}$  NMR spectroscopy ( $\delta$  19.63 and 18.40 ppm for 8 and 8', respectively), the catalytic mixture was considered fully decomposed. The J. Young valve NMR tube was fitted onto a vacuum hookup, and the solvent was evaporated. The tube was then taken into the drybox, and 0.5 g of 1-octene was added to the decomposed mixture. The tube was allowed to stand at 55 °C for 24 h, and the isomer content was determined by  $^1\text{H}$  NMR by integration of the internal olefin peak at  $\delta$  5.40 ppm.

**Acknowledgment.** We thank the National Science Foundation and the Army Research Office for generous funding of this work. K.A.A. also acknowledges the University of Florida for funding of the purchase of the X-ray equipment.

**Supporting Information Available:** Tables giving full crystallographic data for complex 8. This material is available free of charge via the Internet at <http://pubs.acs.org>.

OM0509894

(52) Trnka, T. M.; Morgan, J. P.; Sanford, M. S.; Wilhem, T. E.; Scholl, M.; Choi, T.-L.; Ding, S.; Day, M. D.; Grubbs, R. H. *J. Am. Chem. Soc.* **2003**, *125*, 2546–2558.